

electronics COOLING

FEATURED IN THIS EDITION

**25 DEVELOPMENT OF A 3D
PRINTED LOOP HEAT PIPE**

**30 THERMAL CHALLENGES
WITH WEARABLE
AND IMPLANTABLE
ELECTRONIC DEVICES**

**35 A FIGURE OF MERIT
FOR SMART PHONE
THERMAL MANAGEMENT**

© Copyright 2019 Electronics Cooling

9 CALCULATION CORNER
TRANSIENT THERMAL CALCULATIONS
FOR SKIN CONTACT BY WEARABLE DEVICES

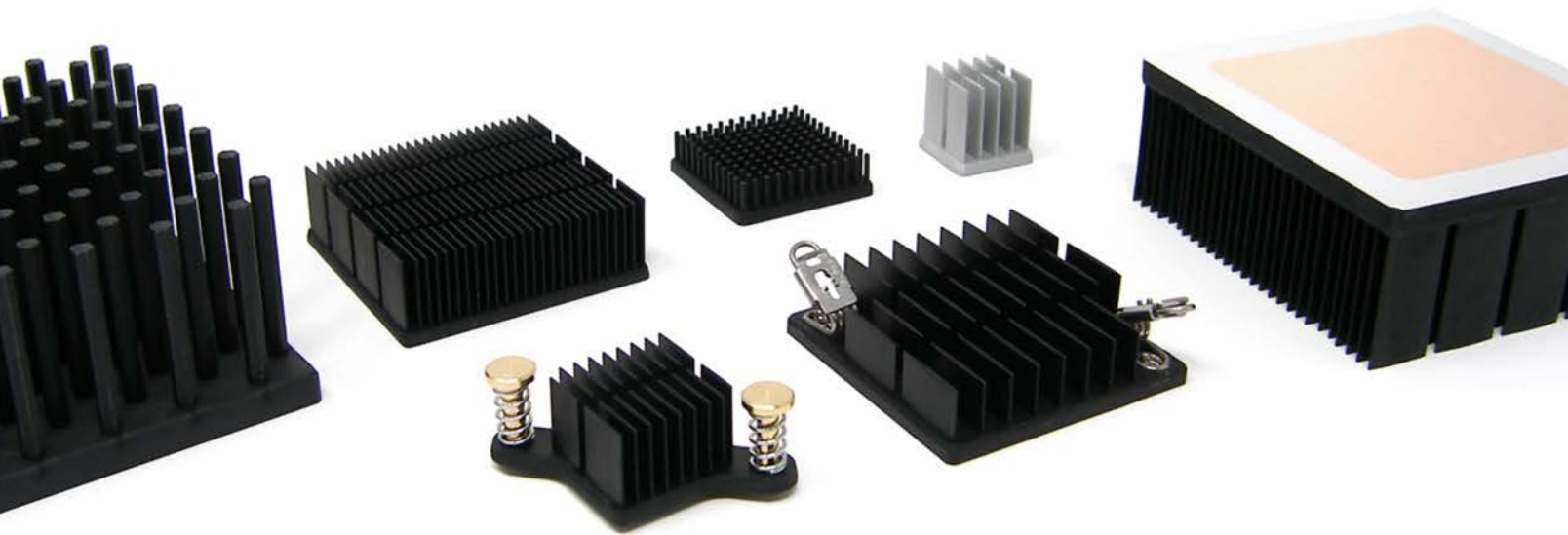
15 THERMAL FACTS & FAIRY TALES
ELECTRONICS COOLING SANITY CHECK

18 TECHNOLOGY CORNER
WHERE WE ARE? WHERE ARE WE GOING?
CHANGES AND CHALLENGES

22 TECHNICAL BRIEF
THERMAL MANAGEMENT AND SAFETY
REGULATION OF SMART WATCHES



Alpha's Extensive Products and Services



Tabbed Push Pin



Push Pin



Shoulder Screw



QuickSet



DC-DC Converter



Optical Transceiver



CPU



LED



Push Pin



Shoulder Screw



Spring



Z-Clip



QSZ Clip



Adhesive Tape



Thermal Interface



Fan

Same Day Shipping

Over 10,000 items with same day shipping.
Heatsinks, attachment hardware and accessories.

Various Attachment Options

Quickset & QSZ anchor pins require Min. PCB area.

Online Custom Design

Custom heatsinks can be designed online.
No MOQ or tooling fees. Lead time is 1-2 weeks.

Copper Embedded Heatsinks

Replacement of heat pipe/vapor chamber.

CONTENTS

- 4 EDITORIAL**
Ross Wilcoxon
- 6 COOLING EVENTS**
News of Upcoming 2019 Thermal Management Events
- 9 CALCULATION CORNER**
Transient Thermal Calculations for Skin Contact
by Wearable Devices
Bruce Guenin
- 15 THERMAL FACTS AND FAIRYTALES**
Electronics Cooling Sanity Check
Ross Wilcoxon
- 18 TECHNOLOGY CORNER**
Where We Are? Where Are We Going?
Changes and Challenges
Victor Chiriac
- 22 TECHNICAL BRIEF**
Thermal Management and Safety Regulation
of Smart Watches
Angel Qian Han
- 25 DEVELOPMENT OF A 3D PRINTED
LOOP HEAT PIPE**
Bradley Richard, Chien-Hua Chen, and William G. Anderson
- 30 THERMAL CHALLENGES WITH WEARABLE AND
IMPLANTABLE ELECTRONIC DEVICES**
Bruce Guenin
- 35 A FIGURE OF MERIT FOR SMART PHONE
THERMAL MANAGEMENT**
Victor Chiriac, Steve Molloy, Jon Anderson,
and Ken Goodson
- 40 COMPANY PRODUCTS & SERVICES DIRECTORY**
- 42 INDEX OF ADVERTISERS**

PUBLISHED BY

Lectrix
1000 Germantown Pike, F-2
Plymouth Meeting, PA 19462 USA
Phone: +1 484-688-0300; Fax: +1 484-688-0303
info@lectrixgroup.com
www.lectrixgroup.com

CHIEF EXECUTIVE OFFICER

Graham Kilshaw | graham@lectrixgroup.com

VP OF MARKETING

Geoffrey Forman | geoff@lectrixgroup.com

EDITOR IN CHIEF

Murray Slovick | murray@electronics-cooling.com

CREATIVE DIRECTOR

Chris Bower | chris@lectrixgroup.com

VP OF STRATEGIC DEVELOPMENT

Ian Quinn | ian@lectrixgroup.com

BUSINESS DEVELOPMENT DIRECTOR

Janet Ward | jan@lectrixgroup.com

PRODUCTION COORDINATOR

Jessica Stewart | jessica@lectrixgroup.com

LEAD GRAPHIC DESIGNER

Kristen Tully | kristen@lectrixgroup.com

PRODUCTION ARTIST

Noah Sneddon | noah@lectrixgroup.com

CONTENT MARKETING MANAGER

Danielle Cantor | danielle@lectrixgroup.com

ADMINISTRATIVE MANAGER

Eileen Ambler | eileen@lectrixgroup.com

ACCOUNTING ASSISTANT

Susan Kavetski | susan@lectrixgroup.com

ASSOCIATE TECHNICAL EDITORS

Bruce Guenin, Ph.D.

Consultant
San Diego, CA
bguenin@usa.net

Ross Wilcoxon, Ph.D.

Associate Director, Mechanical Engineer
Collins Aerospace
ross.wilcoxon@collins.com

Victor Chiriac, Ph.D, ASME Fellow

Principal Architect
Huawei R&D USA
vchiriac@futurewei.com

► SUBSCRIPTIONS ARE FREE

Subscribe online at
www.electronics-cooling.com

For subscription changes email
info@electronics-cooling.com

Reprints are available on a custom basis at
reasonable prices in quantities of 500 or more.
Please call +1 484-688-0300.

All rights reserved. No part of this publication may be reproduced or transmitted in any form or by any means, electronic, mechanical, photocopying, recording or otherwise, or stored in a retrieval system of any nature, without the prior written permission of the publishers (except in accordance with the Copyright Designs and Patents Act 1988).

The opinions expressed in the articles, letters and other contributions included in this publication are those of the authors and the publication of such articles, letters or other contributions does not necessarily imply that such opinions are those of the publisher. In addition, the publishers cannot accept any responsibility for any legal or other consequences which may arise directly or indirectly as a result of the use or adaptation of any of the material or information in this publication.

ElectronicsCooling is a trademark of Mentor Graphics Corporation and its use is licensed to Lectrix. Lectrix is solely responsible for all content published, linked to, or otherwise presented in conjunction with the ElectronicsCooling trademark.

FREE SUBSCRIPTIONS

Lectrix, Electronics Cooling—The 2019 Summer Edition is distributed annually at no charge to engineers and managers engaged in the application, selection, design, test, specification or procurement of electronic components, systems, materials, equipment, facilities or related fabrication services. Subscriptions are available through electronics-cooling.com.

LECTRIX

EDITORIAL

Ross Wilcoxon

Associate Technical Editor



Welcome to the Summer Issue of *Electronics Cooling*[®] Magazine.

I recently saw a LinkedIn post by my friend Jim Petroski. He had provided a link to an article that described a distressing situation in the city of Detroit, Michigan. A few years ago, the city overhauled the city's streetlights, at a significant expense, and installed tens of thousands of LED-based lights. After only a few years, the lights from one vendor began to experience unacceptably high failure rates. Lights from two other vendors are operating without any problems, so the issue is not with the technology but with the design. The defective units were described as either "charred, burned, or cracked" and the picture of a failed unit shown in *The Detroit News* article did nothing to dispel the notion that those lights simply had gotten far too hot. It is always good for me to get the occasional reminders of the critical role that we in the electronics community play in ensuring the performance and reliability of new electronics technologies – and even better when the reminders aren't associated with something that I have personally worked on.

This issue of *Electronics Cooling*[®] has particular emphasis on a topic that personally applies to the majority of our readers: thermal issues related to the electronics that we carry around with us. Thermal engineers are facing increasing thermal management challenges resulting from either miniaturization (evolution from handheld to wearable to implanted) or performance enhancement (our devices become more powerful and integrated). This issue includes two feature articles in this area: one describes a figure of merit for rating the thermal efficiency of handheld devices and the other discusses the thermal requirements for wearable and implantable electronics, with respect to the comfort and safety of the user. This issue also includes a *Technical Brief* and *Calculation Corner* that deal with optimization of the thermal design of a smart watch and the thermal interactions between devices and the skin of the user, respectively.

In addition to this variety of information on personal electronics, this issue of *Electronics Cooling*[®] also includes another feature article that describes very interesting developments in the area of using Additive Manufacturing to fabricate loop heat pipes for small satellites, a new column called *Technology Corner*, which looks at the rapidly evolving technical landscape in the electronics industry, and a *Thermal Facts and Fairy Tales* column aimed at providing readers with a quick way to assess the 'degree of difficulty' of a given thermal problem.

Finally, and most importantly, it is my distinct pleasure to welcome a new member to the *Electronics Cooling*[®] Magazine staff. Starting with our next issue, **Genevieve Martin** of *Signify* will be joining Bruce Guenin, Victor Chiriac and myself as the technical editors. Genevieve is a R&D Manager at Signify (formerly a division of Philips Lighting) where she leads the Thermal Management and Mechanics Competence, manages a team of engineers, and coordinates the EU-supported Delphi4LED program, which includes 15 companies and universities from 7 countries. Genevieve and I have been friends for over a decade, since we first met at the SEMI-THERM and I asked her what she thought of the conference so far. She gave me honest feedback about what she liked and what she didn't... before realizing that I was the Program Chair and might not have actually been looking for that much honesty. I look forward to the insight, energy, experience (particularly in the important area of solid-state lighting), and willingness to say what she thinks that Genevieve brings to *Electronics Cooling*[®].

I hope that you enjoy this issue of *Electronics Cooling*[®] and always welcome your honest feedback on the magazine.

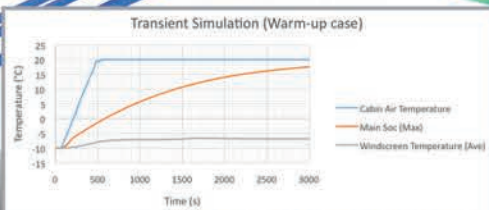
— **Ross Wilcoxon**, *Collins Aerospace*

SIEMENS

Ingenuity for life

Simcenter Flotherm™ XT

- Discover a CAD-centric thermal simulation approach
- Compress the electronics cooling design process by bridging EDA & MCAD design flows
- Accurately model complex shaped geometry with robust automated meshing



COOLING EVENTS

News of Upcoming 2019 Thermal Management Events



26TH INTERNATIONAL CONFERENCE: MIXED DESIGN OF INTEGRATED CIRCUITS AND SYSTEMS

Rzeszów, Poland

The MIXDES conference series started in Debe near Warsaw in 1994 and has been organized annually in different Polish cities. We continue the tradition of choosing the most beautiful and breathtaking places in Poland for the MIXDES venue. This time we invite you to Rzeszów.

The aim of the MIXDES conference is to provide an annual Central-European forum for the presentation and discussion of recent advances in design, modeling, simulation, testing and manufacturing in various areas such as micro- and nanoelectronics, semiconductors, sensors, actuators, and power devices. The MIXDES conference papers are indexed in **INSPEC**, **Web of Science** and available in **IEEE Xplore**.

► <https://www.mixdes.org/Mixdes3/>

SEMICONWEST

Moscone Center, San Francisco, California, USA



SEMICON West is where the industry goes to keep up with developments in a world that is rapidly moving BEYOND SMART — and where it goes to find the information and resources it needs to keep the good times rolling. Three days of presentations with more than 80+ hours of technical and business programming, plus hundreds of exhibitors provide the insights, innovations, and intelligence you need to get ahead and embrace today's disruptive landscape.

► www.semiconwest.org

31ST ANNUAL ELECTRONICS PACKAGING SYMPOSIUM

GE Research Center, Niskayuna, New York, USA



GE Research and IEEC–Binghamton University are proud to host our 31st Annual Electronics Packaging Symposium–Small Systems Integration. We invite you to join us for this two-day event on September 5-6, 2019 at GE Research Center in Niskayuna, NY.

This symposium brings together leaders in academia, industry, and government to discuss the current standing in the field of electronics packaging, and bring value from the varying viewpoints of each respective sector.

► <https://www.binghamton.edu/ieec/symposium/index.html>



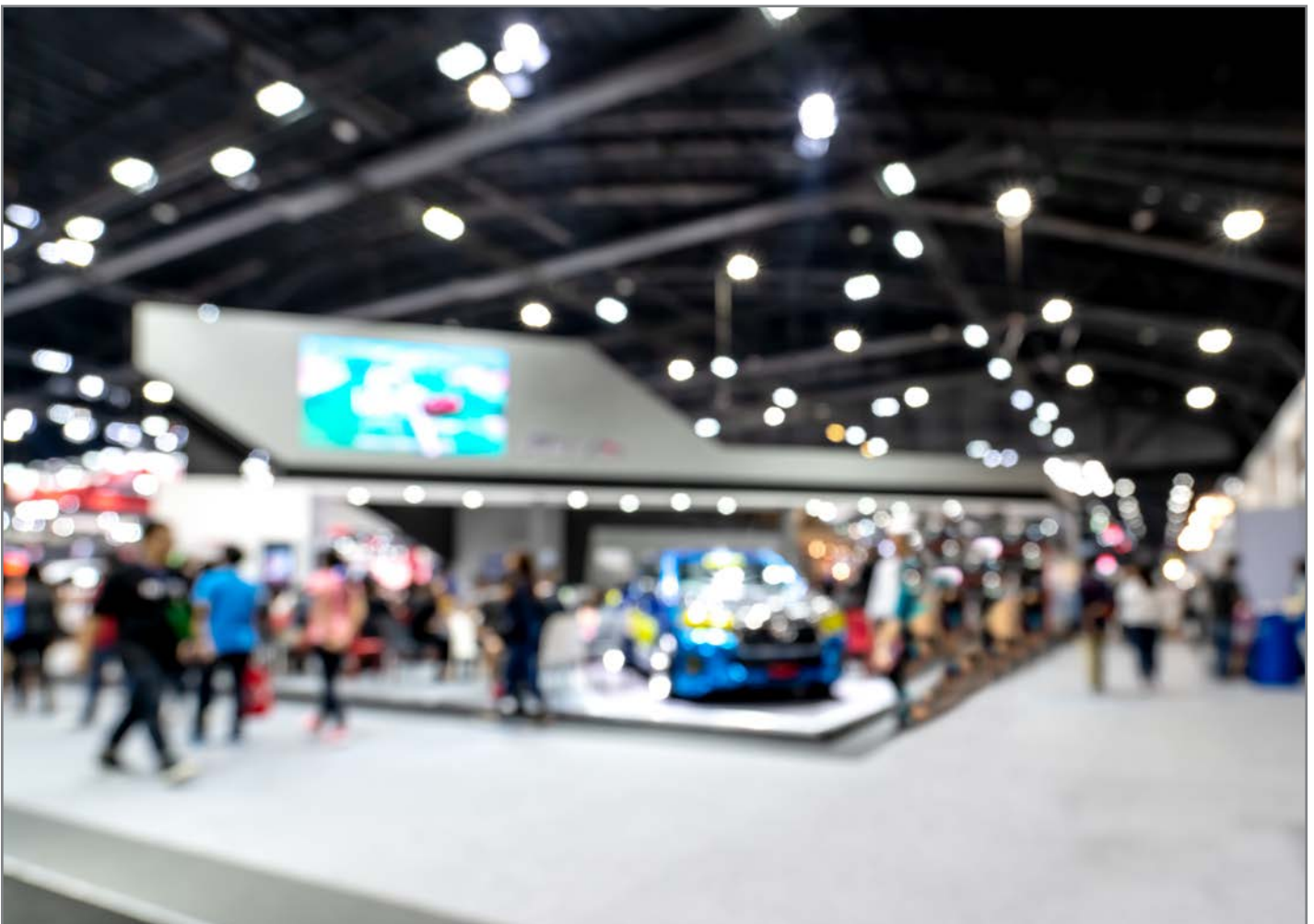
THERMAL LIVE 2019

Online Event

Thermal Live™ is the electronics and mechanical engineer's free, online resource for education and networking in thermal management. Learn the latest techniques and topics directly from thermal management thought leaders without leaving your seat. Join us for two full days of interactive webinars, product demonstrations, whitepapers, and more. Produced by *Electronics Cooling*® magazine.

Available now On Demand: All Thermal Live 2018 Presentations!

▶ www.thermal.live





CALL FOR PAPERS

36th Annual Semiconductor Thermal Measurement, Modeling and Management Symposium
March 16-20, 2020 at the DoubleTree by Hilton, San Jose, CA USA

About SEMI-THERM

SEMI-THERM is an international symposium dedicated to the thermal management and characterization of electronic components and systems. Its goals are to:

- Provide knowledge covering all thermal length scales from integrated circuits to facility levels
- Foster discussions between thermal engineers, professionals and industry experts
- Encourage the exchange of information on academic and industrial advances in electronics cooling

Topics Include: Component/Board/System Thermal Design, Fluid Movers, Acoustics, Advanced Materials, Measurement Methods, Modeling & Simulation, Additive Manufacturing, Reliability, etc.

Applications Include: Processors/ICs/Memory, 3-D packaging, Computing Systems, Data Centers, Portable/Consumer/Wearable Electronics, Power Electronics, Harsh Environments, Defense/Aerospace Systems; Solid-State Lighting & Cooling, Biomedical; Micro/Nano-scale Devices, etc.

Symposium Highlights

Technical Sessions	Technical Short Courses	Tutorials	Vendor Exhibits	Vendor Workshops	Product Tear Downs	Panel Discussions	Poster/Dialog Session
--------------------	-------------------------	-----------	-----------------	------------------	--------------------	-------------------	-----------------------

Three options for participating in the technical program:

Peer-reviewed paper: Submit a full manuscript for peer review in October. Authors notified of acceptance in November. Reviewer comments provided to authors in December. Final manuscript due in January. Manuscripts will be provided to conference attendees.

Non-peer-reviewed paper: Submit an extended abstract (2-5 pages) that describes the scope, contents, key results, findings and conclusions. Authors notified of acceptance in November. Final manuscript due in January. Manuscripts will be provided to conference attendees.

Presentation only: Submit an extended abstract (2 -5 pages) that describes the scope, contents, key results, findings and conclusions. Authors notified of acceptance in November. Final presentation slides are due in March. Presentations will be provided to conference attendees.

Awards: All papers with manuscripts are eligible for the Best Paper Award. Student papers presented at the conference are eligible for Student Scholarships. Presentation-only submissions are not eligible for awards.

Manuscripts and extended abstracts submission deadline	Date that authors are notified of acceptance	Photo-ready full manuscript submission due date
Oct 4, 2019	Nov 15, 2019	Jan 17, 2020

Upload your paper electronically in RTF, DOC or PDF formats at www.semi-therm.org.

For further information please contact the Program Chair

Marcelo del Valle, Thermal Engineer, Intel Americas., E-mail: marcelo.del.valle@intel.com

Visit our website: <http://www.semi-therm.org>

**** All authors qualify for reduced symposium rates ****

Transient Thermal Calculations for Skin Contact by Wearable Devices

Bruce Guenin
Associate Technical Editor

Mobile and wearable electronic devices are truly ubiquitous these days. Thermal engineers involved in the design of these devices are not only attentive to managing the temperature of the various components within these devices, they are also careful to ensure that the temperature on the outer shell of these devices never exceed certain limits as specified in the appropriate standards. These standards exist to protect the user from being burned by routine handling of any electronic device. The risk of burns increases as the device temperature and duration of contact between the device and the skin of the user increase. The graph in *Figure 1* was extracted from a widely used international standard [1] and quantifies these relationships. Furthermore, it highlights the role of the thermal conductivity of the outer shell of the device in influencing the burn risk. It shows that as the thermal conductivity of the device shell decreases, the burn risk decreases also.

It is the objective of this article to provide a deeper understanding of the underlying thermal mechanisms that are operative in the transfer of heat by an electronic device into human skin.

BIO-THERMAL MODEL OF HEAT TRANSFER IN HUMAN SKIN

Figure 2 depicts the flow of heat from an electronic device into the outer layer of skin (epidermis) of the user. The maximum temperature experienced by the user is in this layer. As the heat flows into the deeper layers of skin, it is then convectively removed from the heated region by the body-temperature blood flow from the arteries. The heated blood continues into the veins, whence it flows away from the heated region and is dispersed within the body.

The thermal model framework applied here follows the assumptions in what is widely referred to as the *Pennes Model*. Harry Pennes developed the first bio-thermal equation in 1940 [2]. It took the form of Fourier's heat diffusion equation supplemented by the cooling of tissue by blood flow, which he called "perfusion." He defined perfusion as a linear process in which heat transfer between the blood and the tissue is proportional to the temperature difference between incoming arterial blood and the outgoing venous blood. His model also accounted for the metabolic generation of heat.

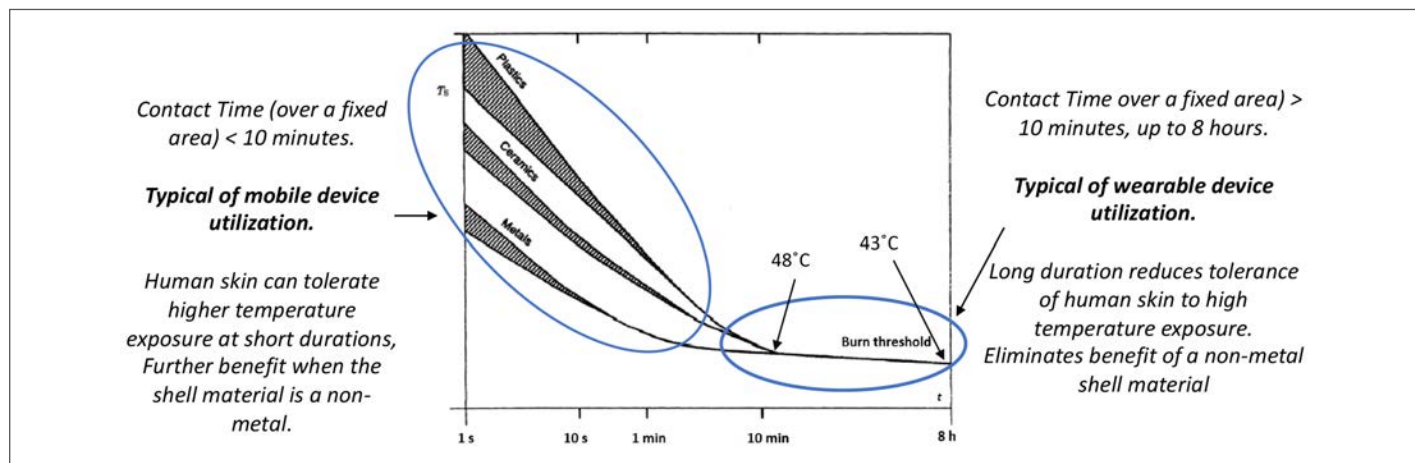


Figure 1 - Burn threshold temperature vs contact time for different device shell materials [1].

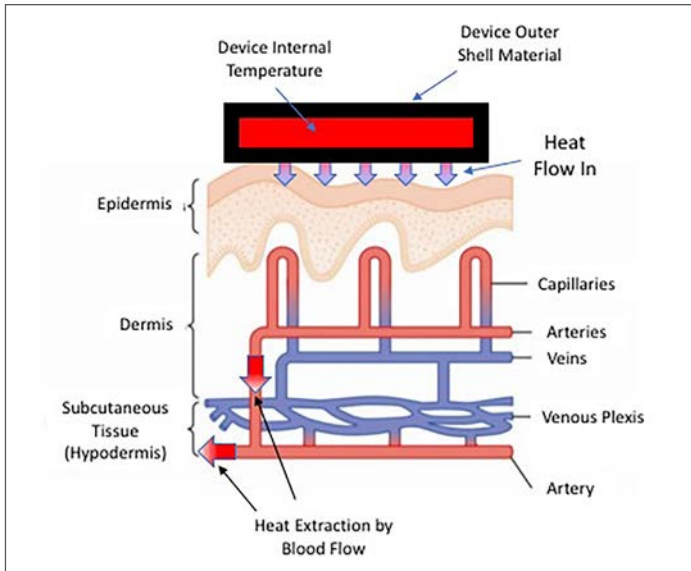


Figure 2 – Heat Transfer from Device Making Skin Contact into Human Tissue

The heat flow situation depicted in *Figure 2* has some simplifying characteristics. To a good approximation, the outer shell of the device is at a constant temperature in the contact region with the skin. Furthermore, the epidermis, dermis, and hypodermis are each thin compared with the width of the contact region and are reasonably constant in thickness. Also, the dermis and hypodermis are uniformly cooled by their own perfusion process. The

net result is that the heat flow is one-dimensional, with a thermal gradient perpendicular to the surface of each layer in the device and skin structures.

As a consequence of these factors, the time-dependent conductive heat flow can be represented by a circuit consisting of linear resistance and capacitance elements. Furthermore, the perfusion heat flow process, being linear, can also be represented by a resistor. This circuit is depicted in *Figure 3*.

TABLE 1					
Material Properties					
Material Class	Material	Thickness	Th.Cond.	Spec. Heat	Perfusion Rate
		(m)	(W/mK)	(J/(m ³ -K))	(1/s)
Skin Layers	Epidermis	8.00E-05	0.1	3.44E+06	0
	Dermis	0.001	0.168	4.54E+06	0.0024
	Hypodermis	0.003	0.168	5.49E+06	0.0024
Device Shell Options	Metal (Al)	0.001	240	N/A	N/A
	Ceramic (Al ₂ O ₃)		17		
	Plastic		0.2		

NOTE: All values of resistance and capacitance of circuit elements assume a cuboidal volume of the indicated thickness and an in-plane area = 1 cm²

Table 1 contains all of the material properties specific to the tissues of interest needed to apply the *Pennes model* [3]. These data were obtained through heat transfer measurements on tissue on

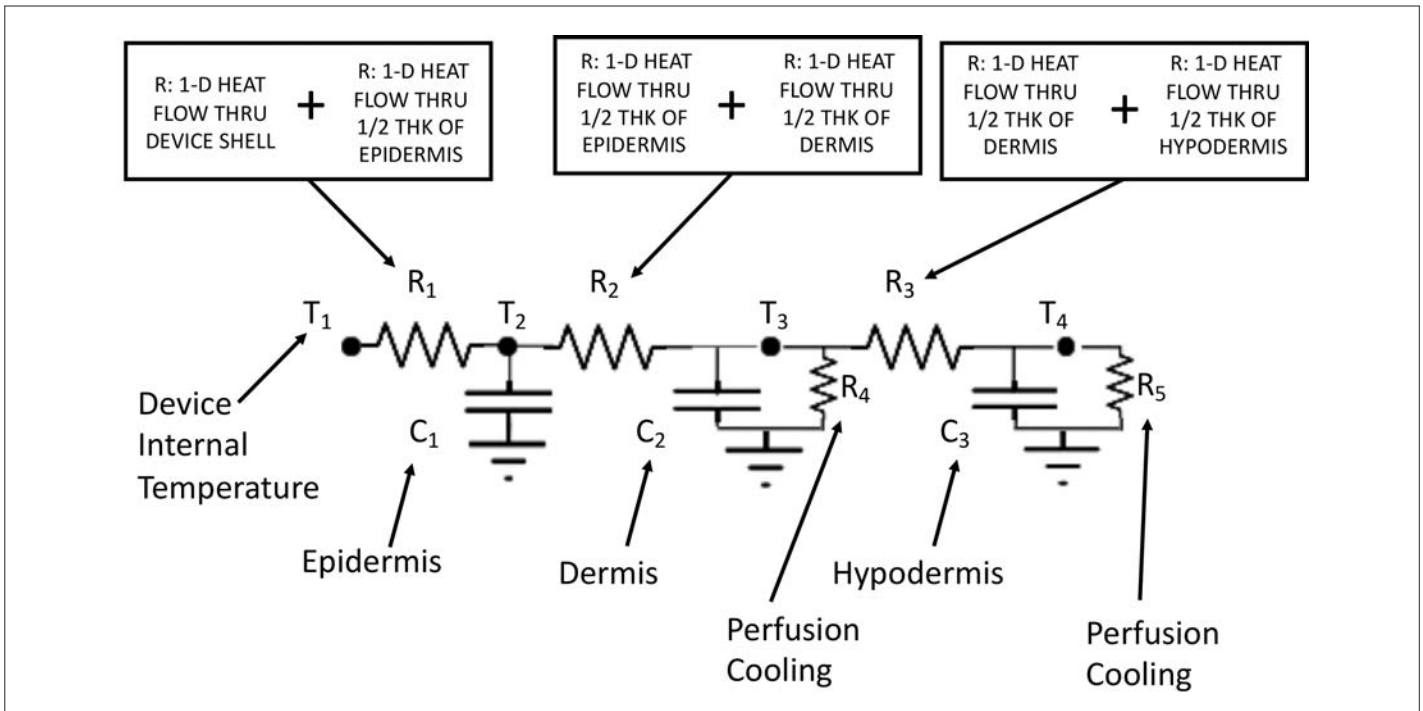


Figure 3 – Lumped element circuit used to simulate transient heat flow from an electronic device in contact with human skin into the various skin layers and then into the blood supply, the result of perfusion cooling.

the underside (anterior side) of the forearm. The relevant properties are the thickness, specific heat, thermal conductivity and perfusion rate for all three skin layers. Note that the epidermis, not having any blood vessels, has a perfusion rate of 0. The dermis and hypodermis have similar values of thermal conductivity, specific heat, and perfusion rate, but differ in thickness by a factor of 3. The epidermis on the underside of the forearm is rather thin, say compared to that on the palms of the hand or the soles of the feet. Its thickness is about one-twelfth of that of the dermis. Furthermore, *Table 1* provides thermal conductivity values of three different device shell materials having high, medium, and low values of thermal conductivity. This enables the simulated results to be compared with the heat transfer behavior implicit in the graph in *Figure 1*.

Table 2 provides the thermal resistance of all the R elements associated with conductive heat flow through each layer of skin and the shell of the electronic device (for each of 3 different shell materials having high, medium, and low thermal conductivities).

TABLE 2		
Thermal Resistance* per Each Material Layer		
LAYER	THERMAL RESISTANCE	
	SYMBOL	*C/W
Epidermis	R,epi	8.0
Dermis	R,derm	59.5
Hypodermis	R,hypo	179
Shell: Metal	R,shell	0.04
Shell: Ceramic		0.59
Shell: Plastic		50.0
*Representing thermal conduction		

They are calculated using the usual formula for 1-D heat conduction:

$$R_{CONDUCTIVE} = \frac{\text{thickness}}{\text{width}^2 * \text{thermal conductivity}} \quad (1)$$

Note that these R values are not the final ones used to represent conduction heat transfer in the circuit. The reasoning is as follows: There are 4 nodes associated with temperature at various locations in the modeled structure. T_1 is the temperature at a node located at the *inner surface* of the device shell and is user-specified. The other three temperatures, namely, T_2 , T_3 , and T_4 , are calculated during the solution process and represent the average temperature in each layer of skin. In a 1-D heat flow situation, their associated nodes are located at the *mid-plane of each cuboid* representing a particular layer. The resistors, R1, R2, and R3, are, therefore referred to as “lumped” elements whose values represent combinations of resistances specific to particular material layers as indicated by the various caption blocks in the figure. *Table 3* provides the calculated values for R1, R2, and R3.

TABLE 3			
Lumped Thermal Resistance Values			
SYMBOL	CALCULATION	SHELL MAT'L	RESISTANCE VALUE
			*C/W
R1	R,shell + 1/2 R,epi	Metal	0.04
		Ceramic	0.59
		Plastic	50.00
R2	1/2 R,epi + 1/2 R,derm	N/A	33.80
R3	1/2 R,derm + 1/2 R,hypoderm	N/A	119.00

The capacitance values (C1, C2, and C3) and the two resistor values associated the perfusion cooling process (R4 and R5) are provided in *Table 4*. Their calculation involves the following two formulas.

$$C = \text{Specific Heat} * \text{Density} * \text{Volume} \quad (2)$$

and

$$R_{PERFUSION} = 1 / (w * \rho_b C_b * V) \quad (3)$$

Where w = perfusion rate (1/sec), ρ_b = density of arterial blood, (1060 kg/m³), C_b = heat capacity of arterial blood (3770 J/kg-K), and V = volume of region to be cooled (m³) [3].

TABLE 4					
Circuit Elements Associated with the Volume of Each Skin Layer					
LAYER	VOLUME (m3)	HEAT CAPACITY		R,PERFUSION	
		SYMBOL	(J/°C)	SYMBOL	*C/W
Epidermis	8.0E-09	C1	0.0275	N/A	N/A
Dermis	1.0E-07	C2	0.5	R4	1043
Hypodermis	3.0E-07	C3	1.6	R5	348
Assumes a cuboidal volume with an in-plane area = 1 cm ²					

An iterative process is used to calculate the time-dependent values of temperature at all nodes in the thermal network. It has been used in the solution of transient behavior involving heat flow in semiconductor components and also moisture diffusion in circuit boards [4, 5].

Several temperatures were assigned to specific nodes before beginning the calculation. They are: 1) temperature of the inner surface of the device shell, set to 49°C, somewhat arbitrarily and 2) the temperature at the “ground” nodes. These were all set to 37°C, a typical value of arterial blood temperature for a healthy adult.

RESULTS

Figure 4 (see below) has two plots for each shell material option, a short duration one on the left and a longer duration one on the right. Overall, the graphs show temperatures for each of the three skin layers. In all cases, the epidermal layer had the highest temperature and the shortest time constant.

Short Duration Plots

As the thermal conductivity of the shell increased, the rise time decreased and the magnitude of the initial rise tended to also increase. With the metal and ceramic shells, the rise time was 0.017 and 0.04 seconds respectively, for them to reach a temperature equal to 90% of the total rise. On the other hand, for the plastic shell, it took 1.1 seconds to it to reach a temperature equal to 90% of the initial rise. This is consistent with the behavior exhibited in *Figure 1* for short duration exposures. Note that with all the shell materials studied, there was only a small change in the temperature of the dermis and hypodermis layers during the time of the initial transient.

Long Duration Plots

The plots representing the behavior with the metal and ceramic shell materials look very similar. At the end of the 14 second duration chosen for these graphs, the temperature for both the dermis and hypodermis layers increased by roughly the same amount, with the dermis temperature reaching one-half of the temperature

rise of the epidermis layer. In this same period of time, roughly that chosen for the “short-duration” plot with the plastic shell, the epidermis and dermis temperatures increased by roughly one-half of the temperature rise experienced with the metal and ceramic shells. One takeaway from *Figure 1* is that for exposure times in excess of 10 minutes, the thermal conductivity of the shell material ceased to be a significant factor in determining the burn risk. The long duration model results in *Figure 4* for the plastic shell show the temperature of all the skin layers converging to nearly the same value and, by the time 1400 seconds have passed (23 minutes), the epidermal temperature is within a degree of that with the ceramic and metal shell materials. These results are certainly consistent with the longer term behavior of the graph in *Figure 1*.

CONCLUSION

A relatively simple thermal resistor-capacitor network has been developed to account for the increase in temperature of the epidermis, dermis, and hypodermis layers due to contact with the

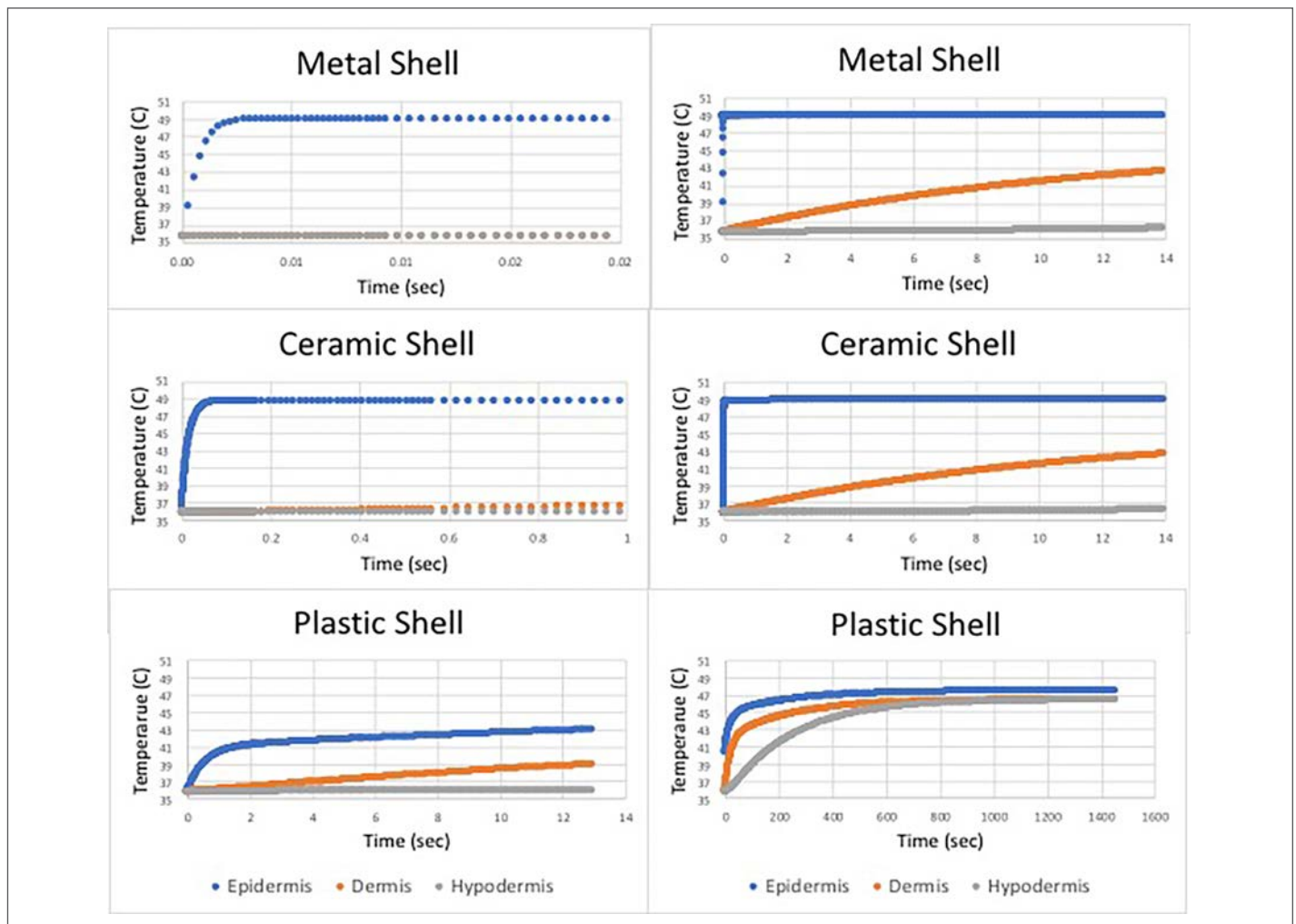


Figure 4 –Thermal simulation results showing the transient behavior of skin layer temperatures due to skin contact with a powered handheld device having an outer shell made of a variety of materials having differing thermal conductivities.

outer shell of an electronic device, for shells of low, medium, and high thermal conductivities. This model has predicted transient behavior involving relative changes in skin temperature that are consistent with those implicit in a leading standards document. Hence, it can provide an understanding of the heat transfer dynamics on the scale of individual skin layers.

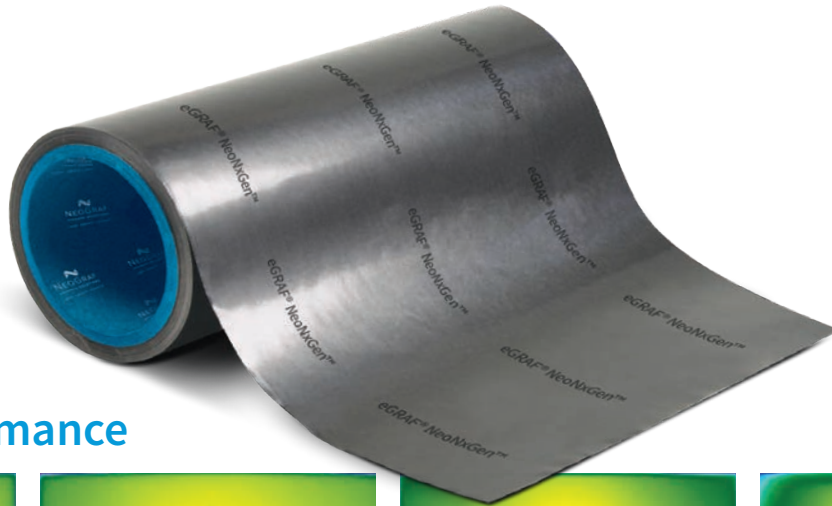
The hope is that this article will give our readers greater insight into the workings of the *Pennes model*, which is widely used in the medical and biological fields, but not yet very much in the electronics industry. Certainly, as wearable electronic devices continue to proliferate, it will become important that thermal engineers become familiar with the *Pennes model* to enable them to add a biothermal component to their device thermal models.

REFERENCES

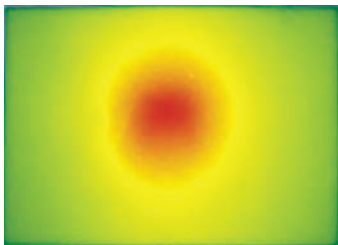
- [1] IEC GUIDE 117 -- Electrotechnical equipment – Temperatures of touchable hot surfaces Appendix A, 2010.
- [2] H. H. Pennes, Analysis of tissue and arterial blood temperatures in resting human forearm, *Journal of Applied Physiology*, 1,(1948) pp. 93–122.
- [3] Maria Strąkowska, *et al.*, “Evaluation of Perfusion and Thermal Parameters of Skin Tissue Using Cold Provocation and Thermographic Measurements,” *Metrol. Meas. Systems*, Vol. 23 (2016), No. 3, pp. 373–381.
- [4] B. Guenin, “Transient Modeling of a High-Power IC Package, Part 1,” *Calculation Corner, Electronics Cooling*, Dec, 2011. <https://www.electroniccooling.com/2011/12/transient-modelling-of-a-high-power-ic-package-part-1/>
- [5] Application of Transient Thermal Methods to Moisture Diffusion Calculations, Part 1,” *Calculation Corner, Electronics Cooling*, Dec, 2012. <https://www.electroniccooling.com/2012/12/application-of-transient-thermal-methods-to-moisture-diffusion-calculations-part-i/>

NeoNxGen™ Thermal Management Solutions

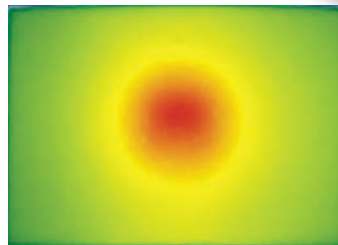
Reduce the Complexity, Not the Thermal Performance



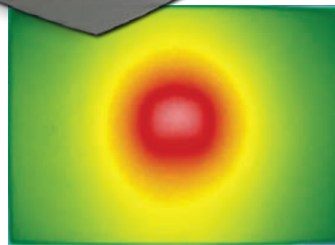
Thermal Performance



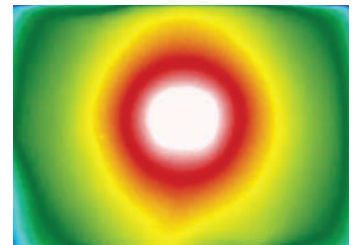
NeoNxGen N-100
100 μm



3-layer 32 μm
Synthetic Graphite
110 μm



SS600-0.102
Natural Graphite
100 μm



Aluminum
100 μm

USED FOR:

Heat spreading to eliminate a hot spot • Shielding a temperature sensitive component
Cooling a hot component

APPLICATIONS:

Consumer Electronics • Transportation • Energy Storage • Medical • Aerospace

When your thermal requirements get complex, your thermal solution doesn't have to.

- > Family of high performance, thick graphite for passive thermal management
- > A reliable, single-layer solution that eliminates the cost, complexity, and reliability concerns of multi-layered graphite solutions

neograf.com

Contact us: info@neograf.com

 **NEOGRAF™**
SOLUTIONS
LEAD. CREATE. CONNECT.

©2019 NeoGraf Solutions, LLC (NGS). This information is based on data believed to be reliable, but NGS makes no warranties, express or implied, as to its accuracy and assumes no liability arising out of its use. The data listed falls within the normal range of product properties, but should not be used to establish specification limits or used alone as the basis of design. NGS's liability to purchasers is expressly limited to the terms and conditions of sale. eGRAF®, GRAFGUARD® and GRAFOIL® are registered trademarks of NeoGraf Solutions, LLC. eGRAF®, GRAFGUARD® and GRAFOIL® products, materials, and processes are covered by several US and foreign patents. For patent information visit www.neograf.com.

Electronics Cooling Sanity Check

Ross Wilcoxon

Associate Technical Editor

A number of years ago I attended a meeting at Purdue University to discuss future challenges and goals for electronics cooling research. One topic that generated a significant amount of interest was, what magnitude of heat flux represented a substantial challenge that the electronics cooling community should be striving to meet with new developments. The closest thing to a consensus that the group could develop was that 1000 W/cm^2 seemed like a pretty lofty goal. I had a difficult time agreeing with this, primarily due to the fact that I was helping with the troubleshooting of a production system that had a heat flux of approximately 1200 W/cm^2 . The primary factor that allowed us to deal with that magnitude of heat flux was the fact that our component was an LED that dissipated approximately 10W but was less than 1mm^2 in size. Clearly, the heat flux alone does not dictate the magnitude of the thermal challenge – the size of the heat source also matters. This becomes obvious with only a little thought; for example, every time we use our cellphone we generate heat flux levels that likely exceed the $10,000 \text{ W/cm}^2$ level – but at the micron-sized scale of integrated circuit junctions.

In a paper that described the LED work [1], I spent a little time discussing the heat flux issue and included a chart that showed examples of how the size of a heat source can influence what constitutes a ‘challenging’ heat flux. I collected data presented at a thermal conference to identify heat flux vs. size data and generated a curve fit that provided some guidance on what constitutes a heat flux ‘limit’ for a given heat source area. This is shown in Figure 1. The fact that the data are plotted on a log-log scale gives it stronger appearance of a good correlation than it likely deserves. But it does seem to show a trend of the heat flux limit being roughly proportional to the inverse of the square root of the heat source area. For the data in this plot, the heat source area is the planform area associated with the heat flux; it does not include enhanced area effects such as from heat sink fins.

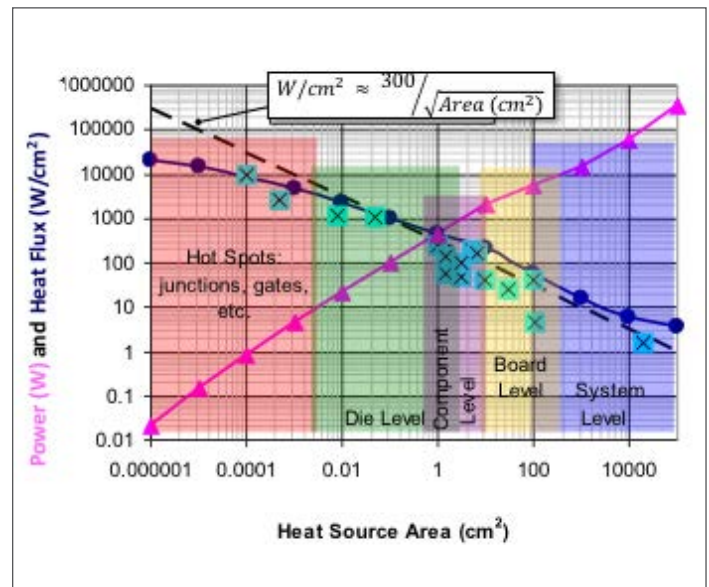


Figure 1 Heat Flux vs. Heat Source Size - General Trends (adapted from [1])

Figure 1 shows that there appears to be a rough relationship between the maximum heat flux (Φ_{limit}) and the size of a heat source (A); namely $\Phi_{\text{limit}} = C^*/A^{1/2}$, where C^* is a constant. The data points shown in the plot were all presented at a conference and appeared to represent challenging, but achievable conditions leading a value of the coefficient C^* approximately equal to 300. This is clearly a rough approximation that can be made even more rough by assuming that other levels of technical challenge would also lead to a specific value of C^* . With this assumption, we can define values of C^* that to correspond to the thermal challenge for a given heat flux and power dissipation in an electronics cooling application. Table 1 shows my attempt at defining values that describe different ‘degrees of difficulty’ for thermal designs.

Thermal Challenge	C*
Fairly easy	1
Reasonable	3
Moderate	30
Challenging	100
Very Difficult	300
Fairly Impossible	1000

Table 1 'Sanity Check' Coefficients for Heat Flux vs. Heat Source Area

Once values of constants have been defined to describe a level of design challenge, one can then assess the difficulty of thermal management for a given combination of power and area. *Figure 2* puts this concept into a graphical form. Based on this chart, a power dissipation of 100 W would be 'fairly impossible' for an area smaller than 0.01cm², 'challenging' for an area of 1cm², and 'reasonable' for an area of ~1000cm².

Before readers cancel their subscriptions to their analysis software and begin basing all future design decisions on *Figure 2*, they should keep in mind the almost breathtaking number, and extent, of assumptions that went into its generation. The chart extends a

very rough regression curve on a limited data set that seems, at best, reasonably representative of electronics cooling applications. But electronics cooling is a relatively broad topic across many industries that have widely varying reliability requirements, ambient temperatures, ambient pressures, types of electronic components, available cooling conditions, types of packaging materials, etc. *Figure 2* ignores the effects of these different constraints to develop a broad generalization. Readers should recall the observation of Alexandre Dumas ("All generalizations are dangerous, even this one") and simply use the figure to develop a sense for how challenging a given thermal condition might be. Better yet, readers may wish to assess their thermal challenges in their own designs, in terms of heat flux and heat transfer area, and use them to define values of C* that correspond to their own experience and create their own version of *Table 1*. Those coefficients can then be used to produce their own version of *Figure 2* that provides a heat flux sanity check that better aligns with their particular design constraints.

REFERENCE

1. Ross Wilcoxon and Dave Cornelius, "Thermal management of an LED light engine for airborne applications", Twenty-Second Annual IEEE Semiconductor Thermal Measurement And Management Symposium, pp. 178-185, 2006

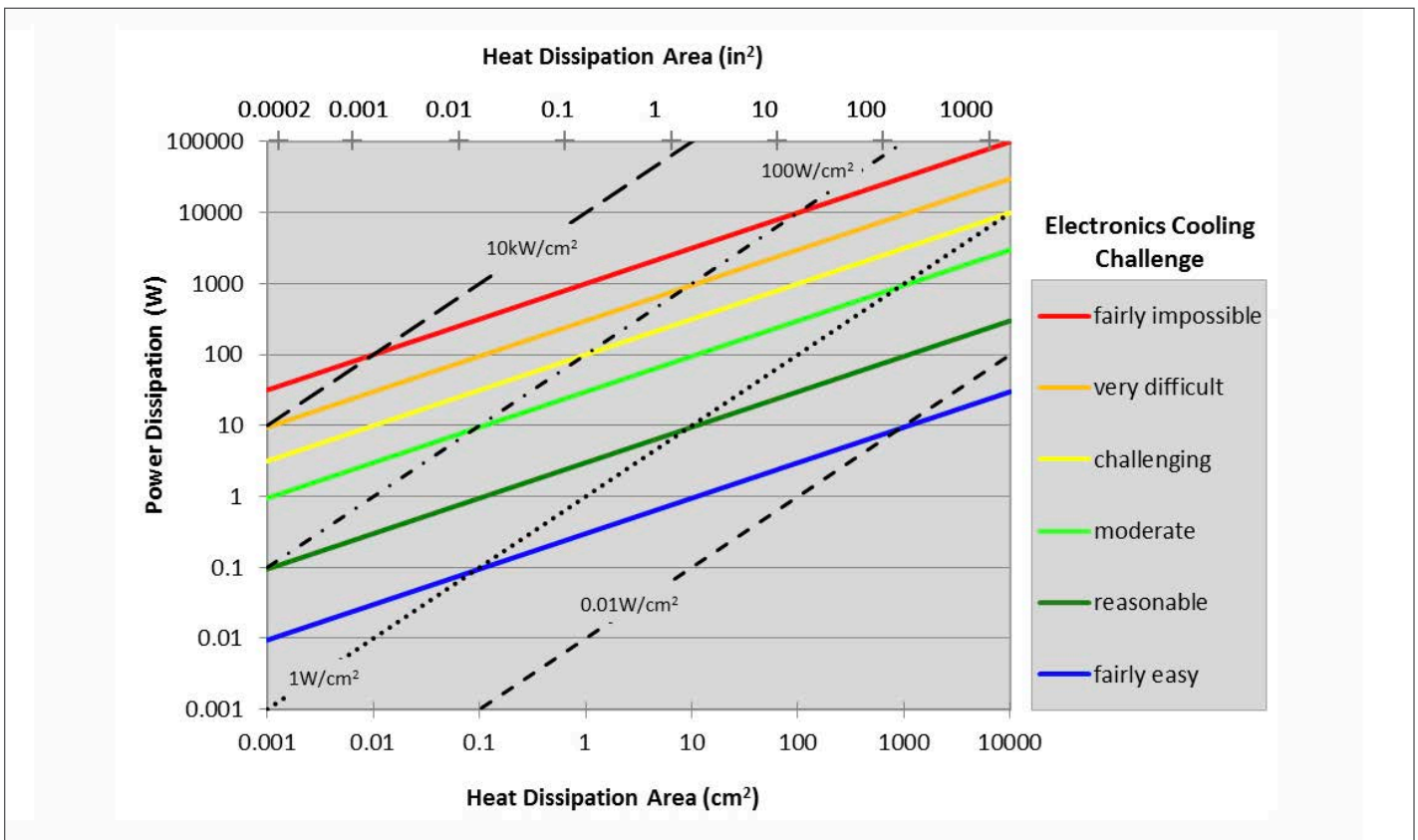


Figure 2 'Sanity Check' Chart for Electronics Cooling

October 22 – 23 2019

thermalLIVE 2019

ONLINE EVENT

The Largest Single Thermal Management Event of The Year - Anywhere.

Thermal Live™ is a new concept in education and networking in thermal management - a FREE 2-day online event for electronics and mechanical engineers to learn the latest in thermal management techniques and topics. Produced by *Electronics Cooling*® magazine, and launched in October 2015 for the first time, Thermal Live™ features webinars, roundtables, whitepapers, and videos... and there is no cost to attend.

For more information about Technical Programs,
Thermal Management Resources, Sponsors & Presenters

please visit:

thermal.live

thermalLIVE
2019

Presented by

electronics
COOLING

Where We Are? Where Are We Going? Changes and Challenges

Victor Chiriac

Associate Technical Editor

It's been an interesting year for the high tech industry in general, and for the semiconductor industry in particular. We have seen the emergence of new technologies and high-tech trends, along with various shifts in the global tech leadership in the chip and mobile industries. I will provide my personal view of the changes and challenges in 2018 and more recently in 2019 as inspired from various personal discussions with industry leaders and veterans and also fueled by various publications and tech related articles... I also plan to touch upon some of the great opportunities lying ahead for the technology landscape as we move further into 2019.

2018 has been a year of transformational change on multiple fronts. We are at the crossroads of what can be called the fourth industrial revolution, where the emergence of several technologies, including hyper-connectivity, advanced telecommunication avenues, Artificial Intelligence (AI), Internet of Things (IoT), cloud computing and big data have led to a dynamic industrial, economic and social environment. There is a call for reinvention happening across the industry that affects companies, society and ultimately our lives. We see how traditional industries are merging and evolving together – for example the growing ties between the automotive industry and the computing, telecommunication industries are creating a renewed environment for growing business success. The technology advancement could be both a democratising force by providing economic and social access to billions, as well as crucial in preventing and managing humanitarian disasters, but conversely has the potential to increase the digital divide and centralise economic and political power.

As experienced by each of us, our daily lives are changing at a very fast pace, with connectivity and mobility driving every aspect of

it. There were approximately 14 billion connected devices in 2015, and that number is expected to double by 2025. Concurrently, the volume of data is expected to reach up to 200 zettabytes by 2025. That is a tenfold increase to the 20 zettabytes in 2016! This is quite significant and with the industry keeping the high performance computing trend line, new innovation and new technologies are at the forefront of this huge growth. And everything requires higher performance, more data, faster processors with thermal/cooling at the epicenter of it all!

We are living at a time where Moore's Law is slowing down as scaling becomes more difficult. The notion that the processing power of computers doubles every two years has hit its limits. Alternatively, companies are accepting the slowing pace of Moore's law but deny its death by looking at alternative measures using 3D chip stacking and other advanced options. *Figure 1* shows the slowing trend in Moore's Law [1]. Innovation in design and architecture to power new devices is critical to keep powering the new devices. Heterogeneous Computing now involves the central processing units (CPUs), the graphics processing units (GPUs), high speed interconnects and other elements that push forward the computing industry... New players in this area emerge every day and the pace of the telecom/computing industry has grown significantly just in the last 6-9 months. One thing is sure - we are living in exciting times!

The significant changes occurring in the very near past continue to amaze. For example, in the last 2-3 years, one of the giant semiconductor companies has repeatedly delayed its move to 10 nanometers (nm) and decided to increase the time between future generations [2]. However, the significant growth of the mobile industry has led to the need for 10 nm and even more advanced technology

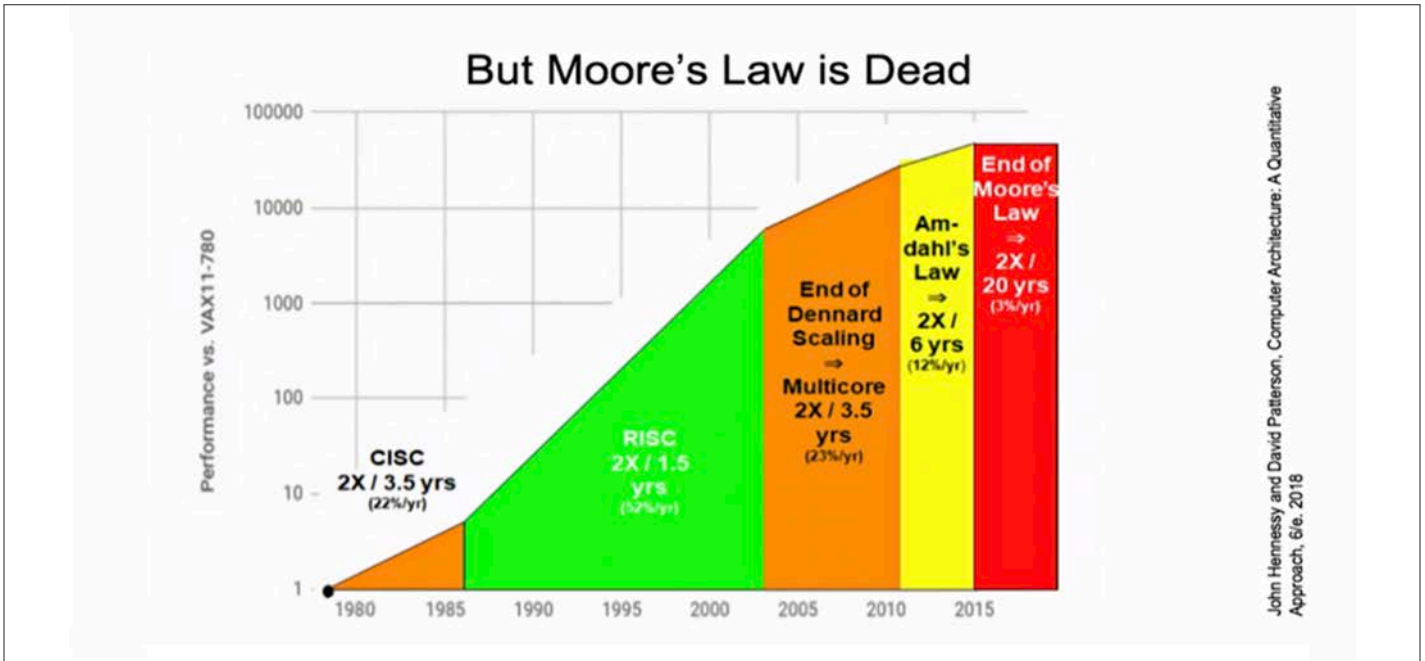


Fig. 1: Moore's Law is slowing. (Computer Architecture, by John Hennessy and David Patterson [1]).

to achieve the needed performance density; as a result, the bulk of the mobile devices are powered by chips made by other companies.

The industry sees significant benefits of lower power consumption at lower technology nodes but doesn't get as much of the cost savings as in the past. The chip expense may rise further as the manufacturing process requires more complex equipment. As the

technology nodes shrink, so does the number of players in the manufacturing field. Consistent with the increased manufacturing costs, reduced revenue and escalating capital costs, so is the distribution of manufacturing. There were over 20 manufacturers at 130nm, but just 5 manufacturers at 22/20nm and 4 at the 14nm node. And we'll continue to see this downward trend. Further details are captured in Figure 2 [3].

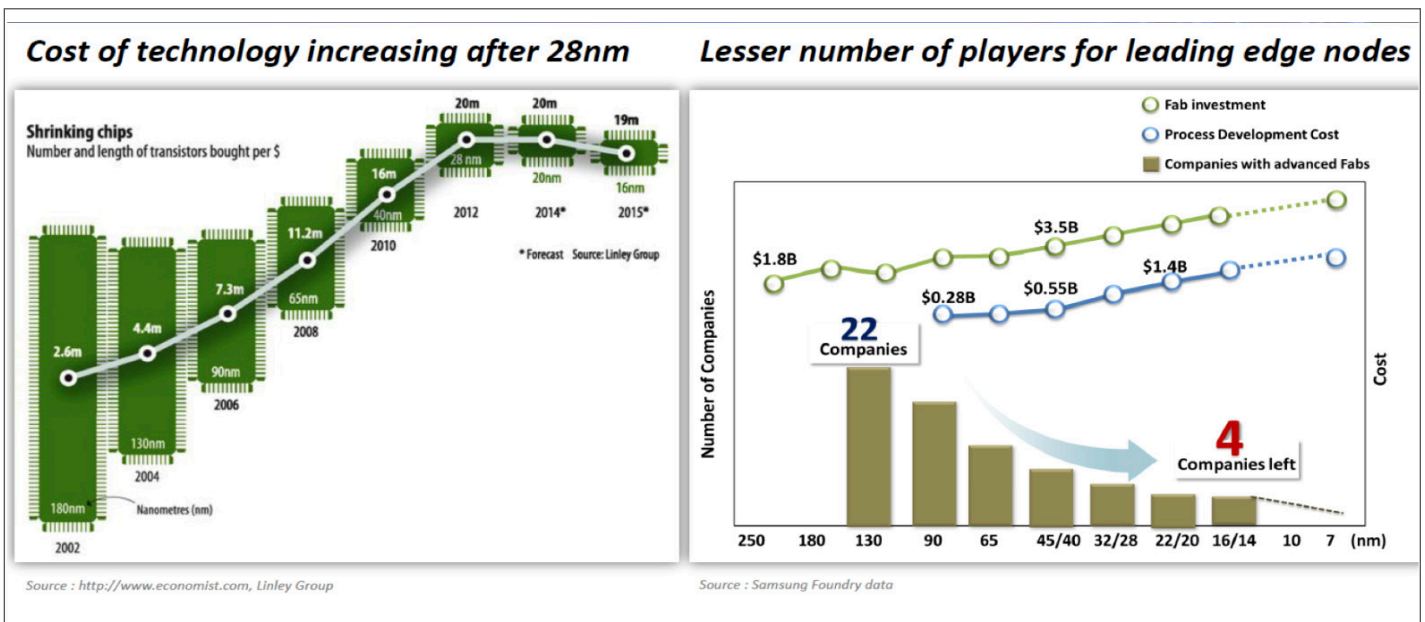


Fig. 2: Increasing Cost of Technology and reduced number of manufacturing companies [3, Fig.1]

With the bulk of the foundry revenue opportunities found at process geometry nodes at or greater than 12 nm, more players shift their focus from investing in 7 nm manufacturing capability and drop out of Moore's Law chase. What does the future hold? It is clear that a range of advanced technologies will provide the key elements of value creation in chip manufacturing going forward. Industry-leading companies will continue to invest in leading-edge process geometries for the benefits they can deliver in memory, processor, and advanced logic solutions [4].

Innovation is the life blood of the semiconductor industry. If Moore's Law—the main driver of manufacturing innovation going back to the earliest days of the chip industry—is reaching the end of its path, it is critical that new technologies be identified that can fuel the continued progress of the industry. Although some have declared Moore's Law to be over or to have slowed down considerably, materials scientists continue to find ways of stretching today's silicon transistor technology while looking for alternatives, such as super thin sheets of carbon graphene and other advanced materials in the next 3-5 years. The landscape is also bound to change in the server market, where the major players will have to get creative to increase the computing power. Alternative ways to improving the design of chips include making specialized chips to accelerate specific/particular crucial algorithms.

To change gears a bit, let's focus on the significant events occurring in the mobile environment. A clear shift has occurred in the past year in the industry and we can see traditional companies changing their strategies to remain competitive in this challenging mobile environment.

Technology advancement is important in many aspects: in the race for 5G, the giants are growing or fading away. The growth/decay cycles are now so fast that any misstep could impact severely the market share and the business health of competing companies in the mobile communication sector. There is clearly an inflection point happening in the mobile and computing industry in general – the rules are changing. Connectivity and battery life could make or break a company. The race for faster devices, faster webpage loading, media editing, improved streaming and higher graphics performance and 4K High Dynamic Range (HDR) is ongoing.

Another trend of the last few years - the social media giants are getting high tech savvy. Social media providers are placing their bets on new Virtual Reality (VR) "all-in-one headset" devices that will solve some of the current VR shortcomings [5]. There may be more...The VR hype is below its prime of the early 2012 - 2013 when it caught on with gamers, tech enthusiasts and others; but with renewed momentum - and with more advanced cooling solutions for the more powerful headsets - we may see a significant growth in this area.

These are the times needed to solve the world's toughest and most interesting challenges, including but not limited to: a) large scale simulations; b) climate change; c) education; d) energy solutions;

e) computational biology, f) disease prevention and I will add here - advanced technologies for the cooling of all of these!!! Other exciting developments are related to the change in computing. As announced earlier this year, the very first operational quantum computational system, which requires cryogenic temperatures, was introduced. Thermal sciences are needed!

And last, but not least - there is the 5G hype - the next G generation will be transformational for our lives allowing the exchange of large amounts of data between us and the environment. 5G is the next generation of wireless communications, providing connections that are at least 40 times faster than the previous 4G-Long-Term Evolution (LTE), with average download speeds around 1GBps.

5G technology may use a variety of spectrum bands, including millimeter wave (mmWave) radio spectrum, capable of carrying large amounts of data a short distance. The drawback of the higher frequencies is that they are more easily obstructed by walls, trees, and negatively impacted by bad weather. As the 5G technology market comes into focus, a number of technologies emerge as vital to the 5G experience. These include mmWave technology; small cells; massive multiple input, multiple output (MIMO); full duplex; software-defined networking (SDN); and beamforming [6]. With the significant growth of the data exchange enabled by 5G, there is greater need for data security and protection. The number of mobile malware apps is growing every year and it is impossible for human analysts to keep up. Various companies and universities are using artificial intelligence and deep learning to hunt for malware in mobile apps. Custom deep neural networks learn to identify malware by scanning the code of tens of thousands of malware apps - far more than any person could ever examine. Using the GPU in all mobile phones, the deep neural networks can scan thousands of apps per-second. The most advanced neural networks run stand-alone on the end user's mobile device, without needing a network connection.

Ultimately, it is anticipated that the 5G networks will help power a significant rise in IoT technology, providing the infrastructure needed to carry huge amounts of data, allowing for a smarter and more connected world - enabling Smart Cities, connected roads, advanced transportation (Self-driving cars), AI robotics, Digital healthcare), smart Sports (athlete training, smart venues, eSports), and so many other. With development well underway and testbeds already live across the world, 5G networks are expected to launch across the world by 2020, working alongside existing 3G and 4G technology to provide speedier connections that stay online no matter where you are.

To conclude, the future involves innovative change. There is an ongoing race for talent. Every AI product or technology of the future must be cyber risk free, have transparency, must improve our lives, must keep the planet clean. Global views on liberty, data use, innovation need to be unlimited, to promote partnerships between government and private practices.

REFERENCE

- [1] John L. Hennessy and David A. Patterson, *Computer Architecture: A Quantitative Approach, 6th edition* (Morgan Kaufmann Publishers, San Francisco, 2017).
- [2] Tom Simonite, "Intel Puts the Brakes on Moore's Law", <https://www.technologyreview.com/s/601102/intel-puts-the-brakes-on-moores-law/>, MIT Technology Review, March 23, 2016.
- [3] Zvi Or-Bach, "28nm Was Last Node of Moore's Law", <http://www.monolithic3d.com/blog/28nm-was-last-node-of-moores-law>, August 29, 2016.
- [4] Dale Ford, "GlobalFoundries Highlights Path Forward as Moore's Law Ends", <https://www.sourcetoday.com/industries/globalfoundries-highlights-path-forward-moores-law-ends>, September 28, 2018.
- [5] Ian Sherr, "Facebook's Oculus Quest heralds VR's next gen, but will we buy in?" <https://www.cnet.com/news/facebook-oculus-quest-heralds-vrs-next-gen-but-will-we-buy-in/>, May 1, 2019
- [6] 5G Technology Promises Faster Connections, Lower Latency, <https://www.sdxcentral.com/5g/definitions/5g-technology/>



Dependable liquid cooling connectors cost less than drips.

Purpose-built to be drip-free, our full line of liquid cooling connectors helps ensure your valuable electronic equipment stays cool and absolutely dry. Our LQ and PLQ Series quick disconnects are ultra-reliable and feature an easy-to-use thumb latch with our audible click to connect. For connections that are worry-free and drip-free, look to CPC.

Learn more at cpcworldwide.com/LQ



Thermal Management and Safety Regulation of Smart Watches

Reprinted from Summer, 2017, issue

Angel Qian Han

Huawei Device USA
San Diego, CA, 92121
qian.han@futurewei.com

ABSTRACT

A smart watch is one of the most popular wearable devices now. Along with battery life and security, thermal safety is the most common concern. We show how to meet the ergonomic standards for users and predict thermal performance in typical scenarios. Thermal simulation software applied at the design stage can provide guidance on the use of heat spreading materials and other thermal solutions to meet the design requirements.

INTRODUCTION

According to the International Data Corporation (IDC) Worldwide Quarterly Wearable Device Tracker [1], by 2019, worldwide shipments of wearables will reach 173.4 million units, resulting in a five-year compound annual growth rate (CAGR) of 22.9%.

Since the smart watch market is relatively young, many concepts of how to integrate electronics are still very new and in the prototyping phase. However, designs are moving in the same direction as mobile phones: engineers must balance performance and high power consumption within very limited space. Customers wear smart watches much longer than they hold smart phones. With greater direct contact with the skin for longer times, thermal comfort is a very important factor in determining the quality of the user experience.

LOW TEMPERATURE BURN AND THERMAL STANDARD

We know that high temperature burns can be very painful and destructive. While burns occurring at low temperature seem to initially be mild and not too painful, they can also cause damage while the victims are less aware that the burn has occurred [2].

In this paper, we suggest values on the lower end of the burn threshold spreads shown in *Figure 1* from the IEC guide 117 for temperature limits of smart watch-based burn risk during operation.

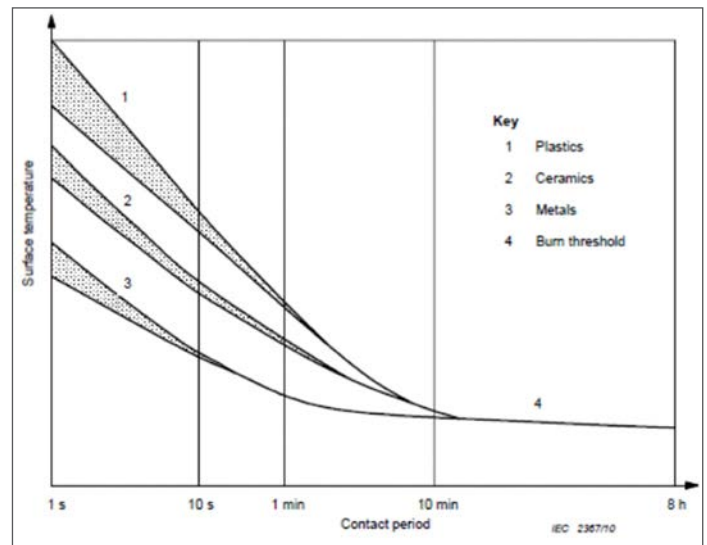


Figure 1. Material temperature and contact period [3]

Temperature limits are different for different time durations. For younger children, short-time maximum temperature limits are lower and stricter. To be more conservative when possible, a smart watch as a heat source that increases skin temperature, which is typically at 32°C, by 3-4 K for days and months will lead to reactions from the body/skin. This local heating will at least feel uncomfortable to the user. The goal is then to maintain the temperatures rise to within 1K for stand-by conditions.

THERMAL MODEL AND TYPICAL SCENARIOS

The smart watch's thermal performance can be simulated with thermal analysis software. The 3D CAD model can be imported to the thermal simulation tool in which boundary conditions can be applied and detailed thermal profile will be obtained.

Material properties of all the components in the model need to be assigned. It is popular to place heat spreaders between high power density chips and the enclosures to reduce the hot spot. Graphite has an anisotropic crystal structure that results in different properties in different directions. This anisotropy can be used advantageously to both spread the heat and to eliminate a hot spot by shielding a surface adjacent to the heat source, as mentioned before. In many cases, metal films made of copper or aluminum can serve as heat spreader in the device.

Scenario 1 is the low power consumption application and the Scenario 2 is the extremely high power consumption application. When the smart watch must process specific functions, the different working cycle and duty cycle value will determine the power consumption, battery usage and thermal profile.

Table 1. Typical scenarios of smart watches			
Scenario	Scenario Description	Working Period	Duty Cycle
Scenario 1	CPU Wake Up	25	120
	Display on	25	
	Accelerometer and sensor running	25	
	Motor vibrator	10	
	GPS search and tracking	25	
Scenario 2	CPU Wake Up	45	120
	GPS search and tracking	45	
	Motor vibrator	20	
	Display on	45	
	Accelerometer and sensor running	45	

TEST RESULTS

The two power level scenarios were studied on a watch prototype. In Scenario 1, the watch case temperature was less than 3°C higher than room temperature, as shown in Figure 2. For the same working period, the longer the duty cycle, the lower the watch case temperature.

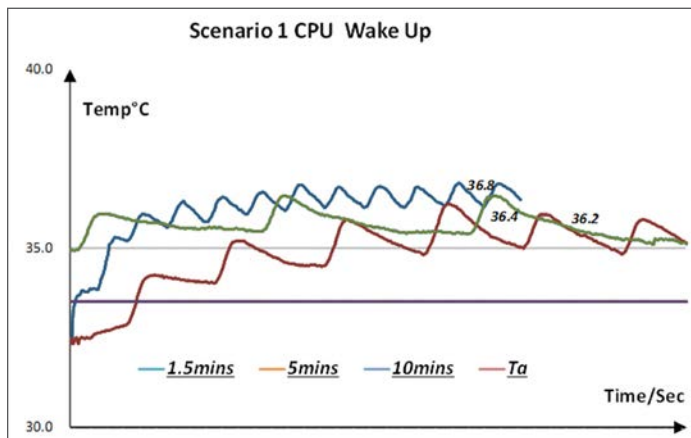


Figure 2. Test result of scenario 1. Test device: Huawei watch prototype, working period 25s, rest period set for 1.5mins/5mins/10mins.

Typical scenarios are closely related to particular design function of a smart watch. Table 1 lists typical product function scenarios.

It is not surprising that the temperature rises in the higher power Scenario 2 were larger than in the low power cases. Figure 3 shows that the maximum case temperature was about 5°C above the ambient air temperature. Figure 2 and Figure 3 both show that the resulting temperature is a function of working period and duty cycle.

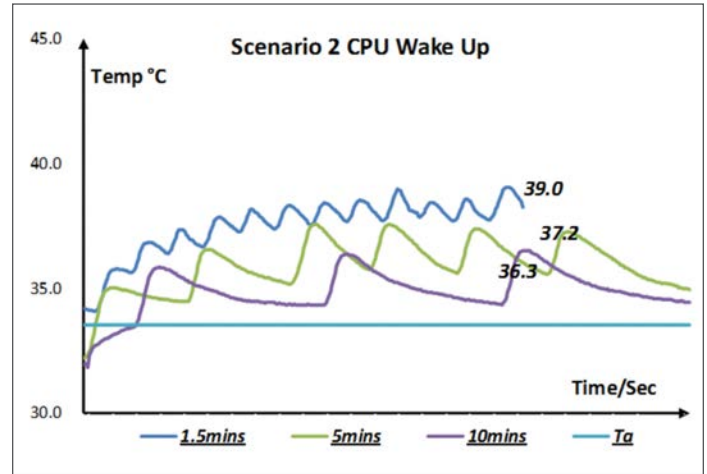


Figure 3. Test result of scenario 2. Test device: Huawei watch prototype, working time as in the table, rest time 1.5mins/5mins/10mins.

The simulation show relatively good agreement with experiment results, the error is below 7% [5].

CONCLUSION

In summary, working period and duty cycle play significant roles in the temperature rise of smart watches. This in turn is a key factor to adjust the power consumption. Thermal solutions, including heat spreading material as graphite and copper film can be applied to reduce the hotspots [5, 6]. Miniature heat pipes [7, 8], are also one of the options for hot spot mitigation. Phase change materials show potential to improving user experience in high power scenarios [9], which can regulate temperature during sprinting [10].

Ergonomic considerations and the device performance need to be well balanced to achieve the best user experience. In smart watch design, maximum inner case temperature is a primary design goal, and perceived performance is more critical than actual performance.

ACKNOWLEDGMENT

The author would like to thank the group members of wearable device to support the marketing investigation, experimental setup and customer survey. Special thanks to Mr. Song Wen and Dr. Jinlinfang, Mr. Kangnanbo and Mr. Kuang Minqiang for their technical comments and related research works.

REFERENCES

[1] International Data Corporation (IDC) Worldwide Quarterly Wearable Device Tracker, 2015

-
- [2] Matthew Seung Suk Choi, Ho Joon Lee, and Jang Hyun Lee, "Early Intervention for Low-Temperature Burns: Comparison between Early and Late Hospital Visit Patients," *Arch Plast Surg.* 2015 Mar; 42(2): 173–178.
- [3] IEC Guide 117, *Electrotechnical equipment– Temperatures of touchable hot surfaces*, Appendix A, 2010.
- [4] Y Hang and H. Kabbani, "Thermal Management in Mobile Devices: Challenges and Solutions" *Proc. of Semitherm 31*, March 16-20, pp46-49, San Jose, CA USA, 2015.
- [5] A. Han, "Thermal management and safety regulation of smart watches", *Thermal and Thermomechanical Phenomena in Electronic Systems (ITherm)*, 2016 15th IEEE Intersociety Conference on, Las Vegas, NV USA 2016
- [6] Smalc, M, G. Shives, G. Chen, S. Guggari, J. Norley, R. A. Reynolds III, "Thermal Performance of Natural Graphite Heat Spreaders", *Proc. of IPACK2005, ASME InterPACK '05*, July 17-22, San Francisco, CA USA, 2005.
- [7] Nguyen, T., M. Mochizuki, K. Mashiko, Y. Saito, I. Sauciu, and R. Boggs, "Advanced Cooling System Using Miniature Heat Pipes in Mobile PC", *IEEE Trans. Component and Packaging Tech.*, Vol.23, No.1, pp.86-90, 2000.
- [8] T. Shioga and Y. Mizuno "Micro Loop Heat Pipe for Mobile Electronics Applications" *Proc. of Semitherm 31*, March 16-20, pp50-56, San Jose, CA USA, 2015.
- [9] Tan, F. L. and C. P. Tso, "Cooling of mobile electronic devices using phase change materials", *Applied Thermal Eng.*, Vol.24, No.2-3, pp.159-169, 2004.
- [10] L. Shao, A. Raghavan, L. Emurian, M. Papaefthymiou, T. Wernisch, M. Martin, and K. Pipe, 2014, "On-chip Phase Change Heat Sinks Designed for Computational Sprinting", 30th IEEE SEMI-THERM Symposium, San Jose, CA USA 2014
-

Development of a 3D Printed Loop Heat Pipe

Bradley Richard, Chien-Hua Chen, and William G. Anderson,

Advanced Cooling Technologies, Inc., 1046 New Holland Ave. Lancaster, PA USA

ABSTRACT

The small form-factor satellites, CubeSats and SmallSats, have increased in popularity and capability, but advanced thermal solutions are required to keep up with the increasing heat loads. Loop heat pipes (LHPs) are a passive solution capable of transporting heat from electronics to deployable radiator panels. However, due to their complicated structure, LHPs require highly skilled workers and labor-intensive manufacturing process that currently make them cost prohibitive for most small satellite applications. The evaporator and compensation chamber account for almost all of the cost of fabrication, which includes sintering, multiple testing and machining steps, and inserting the knife edge seal. To reduce the fabrication cost of LHPs, a wick fabrication via direct metal laser sintering (DMLS) has been developed. This additive manufacturing process significantly reduces fabrication costs by enabling the construction of the primary wick and envelope in an autonomous single step, while also eliminating the knife-edge seal to offer improved reliability.

This article describes a proof of concept LHP primary wick/envelope built via DMLS. A maximum power of 125 W was achieved during steady state testing. Additional tests, including power cycles, adverse elevation, and low power startup, further demonstrate the feasibility of 3D printed LHPs primary wick.

1. LOOP HEAT PIPES

Loop Heat Pipes are passive, two-phase thermal control devices that are used in spacecraft and aircraft thermal control systems. They have been demonstrated to transport up to 1 kW over several meters, in both microgravity and aircraft acceleration. A schematic of an LHP is provided in *Figure 1*. Heat enters the evaporator and vaporizes the working fluid. The vapor passes through grooves in the primary wick and through the vapor line to the condenser. Here the vapor is condensed and subcooled. The subcooled liquid passes through the bayonet tube into the center of the primary wick. A secondary wick allows for communication between the compensation chamber and center of the primary



Bradley Richard

Bradley Richard received his BS in Chemical Engineering from Lehigh University. He has over four years of experience as an R&D Engineer at ACT including work on the design and fabrication of advanced wicks for two phase heat transfer.



Chien-Hua Chen

Dr. Chien-Hua Chen is a Lead Engineer at ACT. Dr. Chen received his BS in Mechanical Engineering from National Taiwan University, and both MS and PhD in Mechanical Engineering from University of Southern California (USC). He conducted his doctoral research in the area of heat recirculating combustion. Dr. Chen has been involved in several high temperature reactor, heat exchanger, and thermal management system development via additive manufacturing process.



William G. Anderson

Dr. William G. Anderson is a Chief Engineer at ACT. He received B.S., M.S., and Ph.D. degrees in Mechanical Engineering from M.I.T. He has been involved in heat pipe, LHP, and pumped two phase cooling at temperatures from 20K (liquid hydrogen LHP) to 2500K (lithium Magnetoplasmadynamic Thrusters), and heat fluxes up to 5,000 W/cm².

wick. The compensation chamber contains saturated fluid at a lower pressure than the evaporator, which provides the driving force for fluid flow. The capillary pressure of the primary wick must be greater than the total pressure drop of the system to pump liquid from the liquid line return to the evaporation site at the vapor grooves [1].

The LHP evaporator wick uses capillary forces to passively supply liquid to the heated surface from the lower pressure condenser. In a heat pipe wick, heat enters from the liquid side of the wick. In contrast, an LHP has an inverted wick, with the vapor located adjacent to the heated surface. LHP wicks are fabricated by sintering metal powder to form a porous body. A typical LHP wick is shown in *Figure 2*. When the wick is inserted in the evaporator, the outer surface of the wick is in contact with the heated surface. Circumferential and axial grooves are necessary to provide flow channels for the vapor to flow to the vapor line. In this case, the axial and circumferential grooves are machined into the wick, although they can alternatively be machined into the evaporator body.

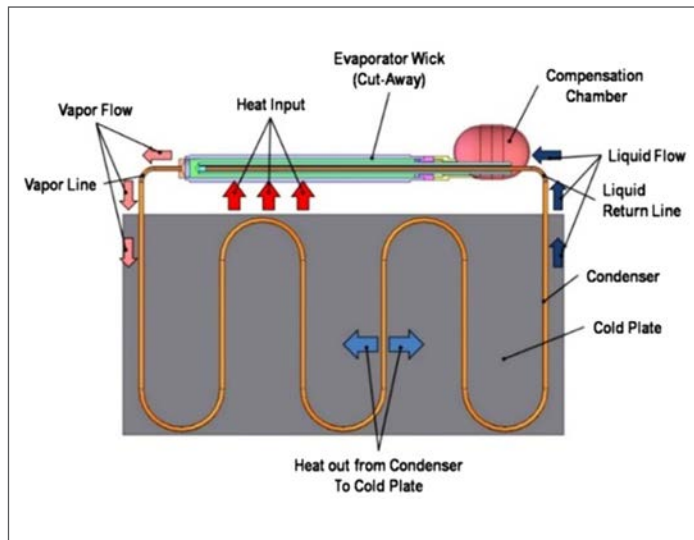


Figure 1 - Loop heat pipe schematic (not to scale).

The evaporator and compensation chamber, shown in *Figure 2*, have a primary wick in the evaporator, and a secondary wick that extends from the evaporator bore into the compensation chamber. The compensation chamber also has a series of screen wicks running from the secondary wick to the walls (not shown for clarity) that allow liquid to be supplied to the secondary wick in microgravity.

During steady-state operation, liquid from the condenser flows through the liquid return line, which terminates near the end of the bore in the primary wick. The liquid then flows back through grooves in the secondary wick, where it is drawn into the primary wick as needed by capillary forces. During unsteady state operation, the compensation chamber acts like a surge tank. If there is more liquid from the condenser than currently needed, the excess liquid flows through the secondary wick into the compensation chamber. If insufficient liquid is available from the condenser, make-up liq-

uid is drawn from the compensation chamber by capillary forces through the secondary wick, and then the primary wick.

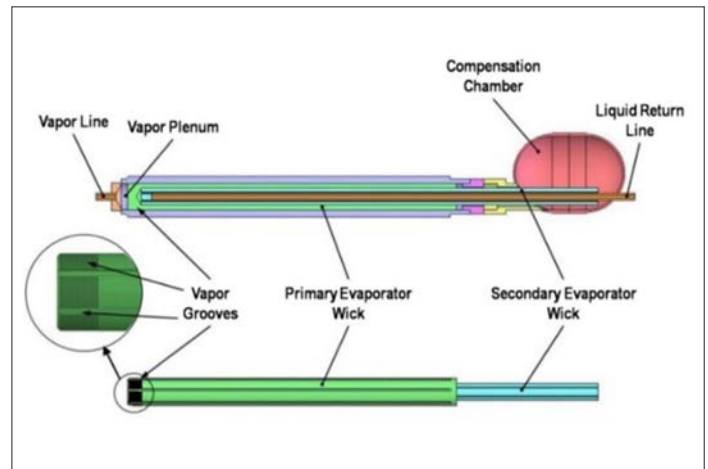


Figure 2. - The primary LHP wick is located in the evaporator. A secondary wick extends from the interior of the LHP into the compensation chamber to supply liquid as needed.

The primary costs to fabricate an LHP are associated with the evaporator and compensation chamber; the remainder is just plumbing [2]. The following steps are required for fabrication:

- Machine the evaporator body, and hone the inner diameter (I.D.) to a very precise dimension.
- Sinter the primary wick. Cut off a small test slug, machine, and measure pore size/permeability to verify the wick properties.
- Machine threaded grooves and axial grooves on the primary wick to remove vapor generated in the evaporator; see *Figure 3*. The liquid return port is also machined, as well as a flat surface for the knife edge seal. Tight tolerances are required on the outer diameter (O.D.) to allow for an interference fit, and on the flat surface to accept the knife edge seal.
- Measure properties on the as-machined wick. If suitable, insert the wick into the evaporator body with an interference fit.
- Measure pore size and permeability after the wick is inserted.
- Fabricate the secondary wick by sintering screen mesh and then machining grooves. Test the secondary wick [2].
- Insert the knife-edge seal, which prevents high pressure vapor in the evaporator grooves from escaping directly into the compensation chamber. Weld to the evaporator and to the compensation chamber.
- Insert the secondary wick into the primary wick, and verify the performance.
- Assemble the complete compensation chamber. Test in a loop to verify functionality.

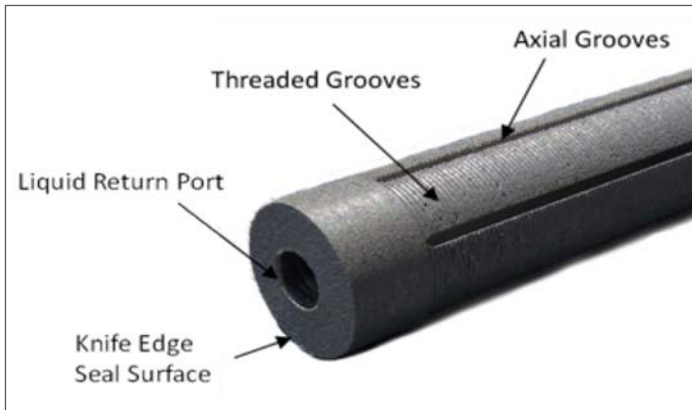


Figure 3. Conventional LHP evaporator wick requires multiple machining and testing steps to fabricate, followed by insertion into the evaporator.

LHPs have been used in many large military, research and communication satellites, in which the cost of the LHPs are only a small portion of the overall satellite cost. CubeSats and SmallSats, which are small form-factor satellites, have increased in popularity and capability, but advanced thermal solutions are required to keep up with the increasing heat loads. CubeSats use a standardized modular design and typically have a mass less than 10kg while SmallSats are a family of small satellites with typical mass in the range of 0.1 to 100 kg [3].

Unfortunately, LHPs made by conventional manufacturing methods are too expensive for small CubeSats and SmallSats. The research discussed below is developing a low cost LHP fabrication process via 3D printing to make LHP feasible for small satellites.

2. 3D PRINTING TO REDUCE COSTS

As discussed, conventional LHPs have been widely used in large, expensive, high-powered satellites and aircraft. Over the last decade, CubeSats and SmallSats are used in increasing numbers due to their low cost, short development times, and increases in capabilities in small satellites. Unfortunately, due to the complex fabrication steps discussed above, conventional LHPs are cost prohibitive for these smaller satellites, many of which are built on a very limited budget.

Using a 3D printed wick and evaporator has the potential to lower LHPs costs so that they can be used in smaller, inexpensive satellites. The DMLS fabrication process will eliminate many of the steps discussed in the last section, since the evaporator envelope and primary wick can be fabricated at the same time. The ability to print solid and porous wick material together in a single part also eliminates the need for the conventional knife-edge seal, which improves reliability.

The performance of an LHP primary wick depends largely on pore size. The capillary pressure of a wick is inversely proportional to pore radius. For successful LHP operation, the capillary pressure must be greater than the total system pressure drop. Therefore, by reducing the pore size of the primary wick, the maximum power

can be increased. Traditionally sintered primary wicks have a pore radius of approximately 1 μm . DMLS has been demonstrated to be capable of printing porous lattice structures, but the smallest pore size to date has been about 50 μm . This is due to the accuracy and precision of the laser as well as thermal stresses and heat spreading.

In this work, a different approach was taken towards 3D printed wick structures. Instead of building a defined lattice structure, the laser power, speed, and spacing were varied to partially sinter the metal powder together instead of fully melting the particles. This results in a wick structure very similar to that of traditionally sintered wicks.

An experimental optimization study was completed by printing a total of 15 samples using a range of DMLS parameters. The goal was to achieve the smallest possible pore size to maximize capillary pumping power. The pore size was measured for the samples, and varied from 5.6 μm to 32 μm . The smallest pore size is capable of providing enough capillary pressure for an LHP in the 100-300 W range. The DMLS parameters for this sample were used for fabrication of the LHP prototype. Achieving smaller pore sizes is likely possible by using smaller diameter metal powder as the base material, but there are no current commercially available solutions [4].

The LHP evaporator prototype is shown in Figure 4. The vapor vents, shown in the evaporator front (top left), are used to feed the vapor generated in the evaporator to the vapor line. They are formed during the 3D printing process.

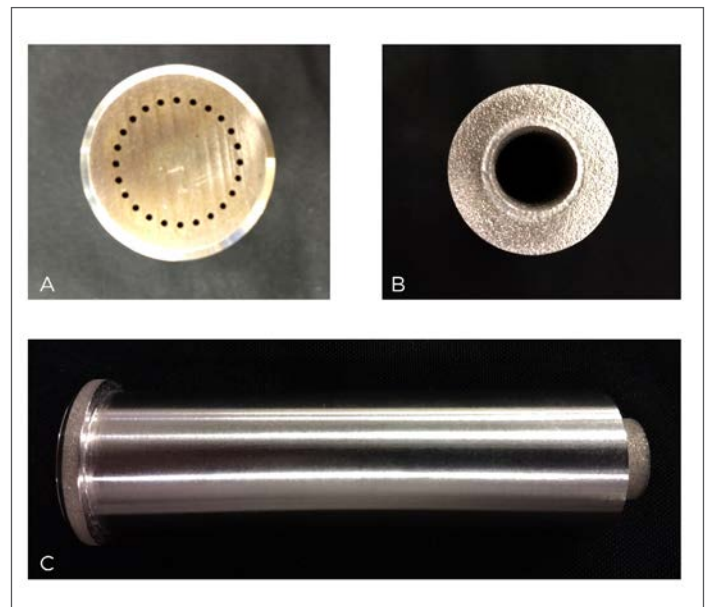


Figure 4: (a) Front of the LHP evaporator, showing the vapor channels. (b) Back of the LHP evaporator. (c) Side view.

The side of the LHP evaporator is shown at the bottom of the figure, and the back of the LHP evaporator is shown in the top right. One of the main advantages of the 3D printed LHP evaporator is the elimination of the many machining and testing steps need-

ed to insert the primary wick. A second major advantage is the elimination of the knife-edge seal, which seals the pressure difference between the evaporator inverted wick and the compensation chamber. In the 3D printed LHP, the printing parameters were simply altered to provide a solid cap above the wick.

3. EXPERIMENTAL DEMONSTRATION

A proof of concept LHP prototype with 3D printed evaporator was built (Figure 5). The working fluid used was ammonia. The primary wick was 2.54 cm in diameter and 10.2 cm in length. The primary wick as printed had a porous interior with a fully dense envelope that was welded directly to the compensation chamber and vapor line. The tubing was 0.318 cm in diameter and the condenser was 99 cm in length. The sink temperature for testing was set to 0°C.

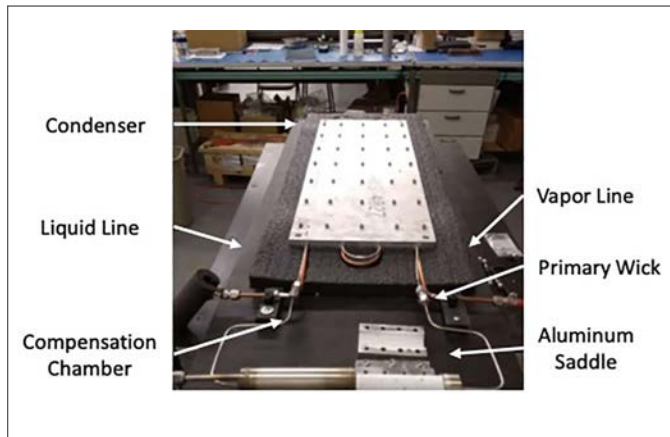


Figure 5: Completed LHP prototype with 3D printed primary wick.

The steady state testing results from the LHP prototype are provided in Figure 6. Startup occurred almost instantly at a power of 110 W, which can be seen by a rapid decrease in the temperature of the liquid line. The power was increased in 5 W increments, and steady state was achieved at a maximum power of 125 W. At 130 W the temperatures of the LHP began to increase linearly which is an indication of dry-out in the primary wick. This power limit can be increased by increasing the length of the evaporator.

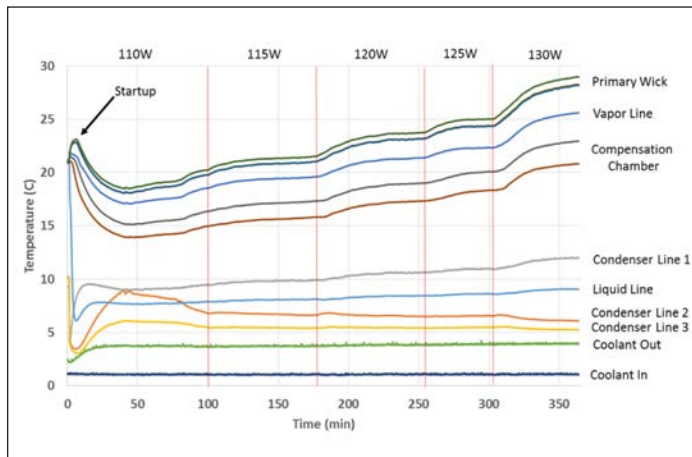


Figure 6: Steady state testing of LHP prototype

	Conventional	3D Printed
Power	1kW	100-150W
Length	3-5 m	1 m
Adverse Height	1 m	20 cm
Pore Size	1 μm	5-7 μm
Wick Machining	Yes	No
Knife Edge Seal	Yes	No
Cost	\$\$\$\$	\$\$

Table 1. Conventional vs. 3D Printed LHPs.

Power cycle testing was completed to verify the ability of the LHP prototype to handle transients. The power was rapidly changed between 70W and 20W. A temperature plot of the results is shown in Figure 7. Dry-out did not occur with rapid increases or decreases in power. This indicates that the secondary wick was able to maintain the supply of liquid to the primary wick during transient operation.

The *HIGHS* & *LOWS*

of thermal management

One Part Cryogenically Serviceable Epoxy System

Supreme 18TC

LOW

Thermal resistance, 75°F
5-7 x 10⁻⁶ K•m²/W

HIGH

Thermal conductivity, 75°F
3.17-3.61 W/(m•K)

WIDE

Service temperature range
4K to +400°F

MASTERBOND®

ADHESIVES | SEALANTS | COATINGS

Hackensack, NJ 07601 USA • +1.201.343.8983 • main@masterbond.com

www.masterbond.com

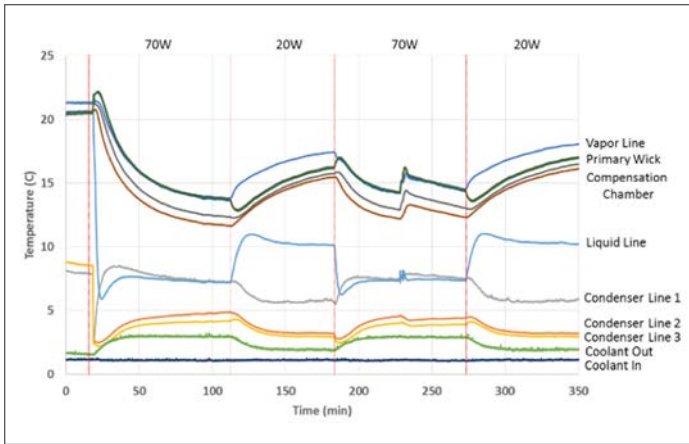


Figure 7: Rapid power cycling between 70 W and 20 W test results demonstrating the ability of the secondary wick to prevent primary wick dry-out during transients.

To demonstrate the ability of the LHP to survive launch, the LHP evaporator was subjected to a vibration test representative of launches. Thermal testing after the vibration test showed no change. Additional testing includes low power startup, and testing with the evaporator tilted at a 25° adverse angle to show that the LHP can operate on Lunar and Martian Landers and Rovers. Details can be found in [4] and [5].

Table 1 compares the properties of conventional versus 3D printed LHPs. The conventional LHPs can carry higher powers over much longer lengths, but are very expensive. 3D printed LHPs can carry less power due to the limitation of current pore size, but still within the range of anticipated CubeSat/SmallSat powers (100 to 150 W). Their greatly reduced fabrication costs make them affordable for these smaller satellites.

CONCLUSIONS

Conventional LHPs are a standard thermal control device for high power military, communication, and research satellites, as well as

aircraft thermal control. Unfortunately, they are too expensive for CubeSats and SmallSats, which are increasing in popularity. A newly developed 3D printed LHP evaporator process eliminates many fabrication steps, dropping the fabrication costs to a range suitable for these smaller satellites. An LHP prototype demonstrated the ability of a 3D printed wick to perform as an LHP primary wick. A maximum power of 125 W was achieved which is in the power range of current CubeSat technologies. LHP performance was also verified for operation against gravity and during rapid changes in heat input power. The next step is to verify operation in microgravity as well as further reducing the pore size to increase the power density via smaller diameter metal powder.

ACKNOWLEDGMENTS

This work was funded by NASA through the Small Business Innovation Research (SBIR) program under contract NNX17CM09C. The technical monitor is Dr. Jeffery Farmer. We would like to thank Joel Crawford and Merryl Augustine for their help in developing the 3D printed LHP.

REFERENCES

- [1] Ku, Jentung. Operating characteristics of loop heat pipes. No. 1999-01-2007. SAE Technical Paper, 1999.
- [2] Anderson, W.G. et al., “Loop Heat Pipe Design, Manufacturing, and Testing – An Industrial Perspective,” ASME 2009 Heat Transfer Summer Conference, San Francisco, CA, July 19-23, 2009.
- [3] “What are SmallSats and CubeSats?,” <https://www.nasa.gov/content/what-are-smallsats-and-cubesats>, accessed May 10, 2019.
- [4] Richard, B. et al., “Development of a 3D Printed Loop Heat Pipe,” Semi-Therm, San Jose, CA, March 18 – 22, 2019.
- [5] Richard, B. et al., “Development of a 3D Printed Loop Heat Pipe,” to be presented as the 49th International Conference on Environmental Systems, Boston, MA, July 7-11, 2019.

Thermal Challenges with Wearable and Implantable Electronic Devices in Healthcare

Bruce Guenin

Associate Technical Editor

INTRODUCTION

Traditionally, medical science has depended on a variety of diagnostic tests administered by medical personnel to either detect the onset of an illness or to monitor its progress. More recently, this focus has been supplemented by a strategy of health maintenance and disease prevention. Both of these strategies benefit from the frequent testing of individuals. Of course, the ideal situation would be continuous sensing of many parameters, highly correlated with the wellbeing of the patient, in a manner that requires no attention or effort on the part of the patient. With the continuing miniaturization of electronic devices, this vision is becoming a reality. There are now devices that are capable of monitoring specific body metrics on a continuous basis. This article explores some of the devices that are providing these functions for us now and also looks at the longer term trends in their development. It also discusses the thermal criteria that are applied to the thermal interaction of such devices with the patient to determine their suitability for use over extended periods of time [1].

EXAMPLES OF ELECTRONIC DEVICES USED IN HEALTHCARE APPLICATIONS

Figure 1 depicts representative examples of mobile, wearable, and implantable devices with a range of capabilities in monitoring and maintaining health. The associated graphs provide a comparison of these devices according to their overall volume and their energy consumption, as represented by the energy storage capability of their battery.

Even though the smart phone doesn't have the same ability as a wearable device in directly sensing different bodily processes such as pulse, movement, and temperature, it functions as an effective interface to the user in aggregating and processing the results measured by wearable and implantable devices and sharing them with the user as well as with any healthcare provider selected by the user.

The transition from mobile phone, to smart watch, to fitness tracker is accompanied by a similar trend in the reduction in the volume of the device and the energy capacity of their batteries. Both the smart phone and smart watch are multi-purpose devices with advanced computational and communication capabilities, having a high-resolution display. The fitness tracker has a much narrower range of capabilities, a simple display, and only Bluetooth communication capability. This results in a smaller size and much less energy dissipation than the smart watch. All these devices have rechargeable batteries and the expectation is that they will be attached to a charger on a daily basis. Any sensing that they do of the user's body functions requires only physical contact with the user and no penetration of the user's skin.

The three devices on the right side of the figure, on the other hand, need to interact with the interior of the user's body. The glucose sensor needs to penetrate the user's skin in order to perform the glucose measurement. The implantable devices, by definition, are inserted into the user's body. Both the glucose sensor and the pacemaker employ single-use batteries, that have to be replaced at regular intervals: on the order of months for the glucose sensor and

The Progression in Personal Electronic Devices: Mobile => Wearable => Implantable

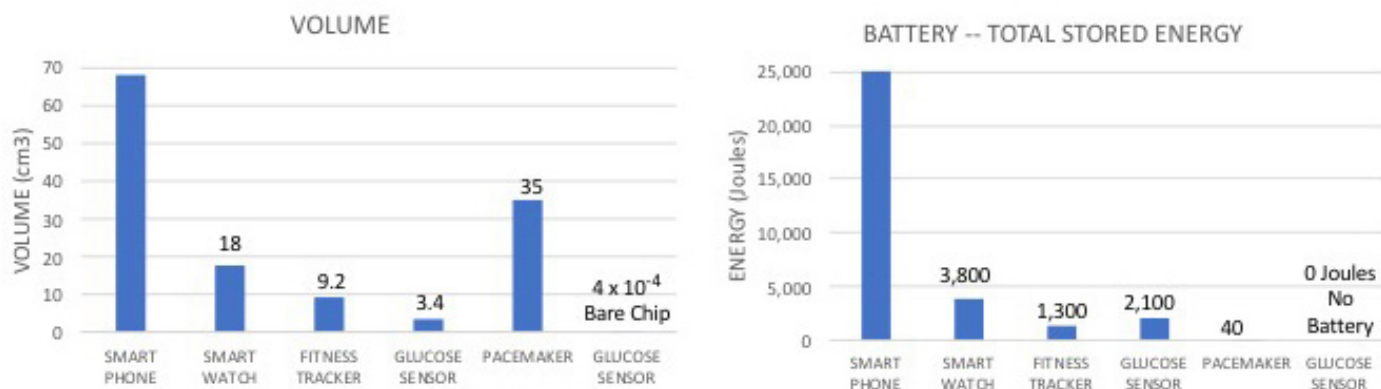


Figure 1

on the order of years for the pacemaker. Hence, the battery capacity for the glucose sensor is larger than that for the fitness tracker, which has more functionality, and therefore higher current draw, but which has the advantage that it can be recharged daily.

The implantable glucose monitor depicted is an experimental prototype and has not yet been commercialized [2]. However, it has features that we can expect to see on other implantable sensors in the future. It is extremely small and can be inserted under the patient's skin with a simple, out-patient procedure. It has no battery. The approach used here was to use radio frequency waves for both remote monitoring of the sensor using Bluetooth and powering it using wireless power transfer. Both the power transfer and Bluetooth signaling could be provided by a single wearable device, located near the implanted device. Such an implanted device could conceivably perform its functions reliably for years and without any maintenance. In this way, it would require no attention by the user.

VARIETIES OF IMPLANTABLE MEDICAL DEVICES NOW UNDER DEVELOPMENT

The pacemaker is arguably the most widely used implantable medical device at the present time. It differs from the other devices shown here in that it actually controls a bodily function, namely the contractions of the heart. It does not simply monitor it.

The following table lists implantable devices now in various stages of development [3]. The ones with a life sustaining impact are intended to prevent episodes of either brain or heart irregularities and have a control function. The other devices serve a sensing function, and enhance the quality of life of the patient by ameliorating either vision or hearing impairment or continuously monitoring various vital signs and alerting the user and healthcare providers when an intervention is needed.

They employ wireless communication for data transmission and in most cases use wireless methods of powering the devices.

TABLE Implantable Devices Now Under Development		
Life Impact	Associated Disease	Device Type
Sustaining	Epilepsy	Brain Stimulator
	Heart Disease	Cardiac Pacemaker
		Defibrillator
Enhancing	Diabetes	Glucose Sensor
	Glaucoma	Intraocular Pressure
	Hearing Loss	Cochlea Implant
	Heart Disease	Blood Pressure Sensor
		Heartbeat Sensor
	Lung Disease	Blood Oxygen Level
Vision Impairment	Retina Implant	

THERMAL LIMITS FOR PORTABLE AND WEARABLE DEVICES

There are many stationary electronic devices in our homes and offices that we deal with on a daily basis. The thermal engineers involved in their design were concerned mostly with the maximum temperature reached by the various electronic components in the device. Normally, the temperature of the cabinet enclosing a device is at a temperature not much higher than room temperature because the internally-generated heat is typically exhausted from the unit by a flow of air. The people in the vicinity of the device might occasionally touch its exterior, but it would be rare that a person's skin would be in contact with it for an extended period of time.

With the introduction of mobile and wearable electronics, there are two notable differences:

- 1) In general, all the heat generated within the device flows via conduction through the outer shell of the device. It is common that the exterior of a mobile device feels warm or even hot to the touch.
- 2) A mobile device can be in contact with the user's hand or ear, etc. for an extended period of time. In the case of a wearable

device, there could be constant contact with the user's skin over a period of days.

Figure 2 depicts the flow of heat from an electronic device into the outer layer of skin (epidermis) of the user. The maximum temperature experienced by the user is in this layer. The heat is then convectively removed from the heated region by the body-temperature blood flow from the arteries. The heated blood continues into the veins, whence it flows away from the heated region and is dispersed within the body.

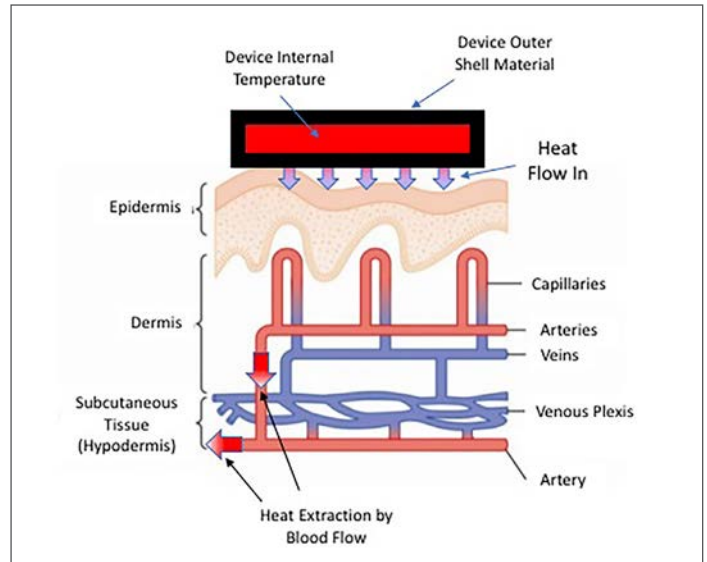


Figure 2 – Heat Transfer from Device Making Skin Contact into Human Tissue

Intuitively, we would expect that the probability of getting a burn from skin contact with an electronic device would depend on the following factors: the temperature of the device and the total time the device has been in contact with a particular region of skin. It turns out that the thermal conductivity of the outer shell of the device is also an important factor. Higher conductivity shell ma-

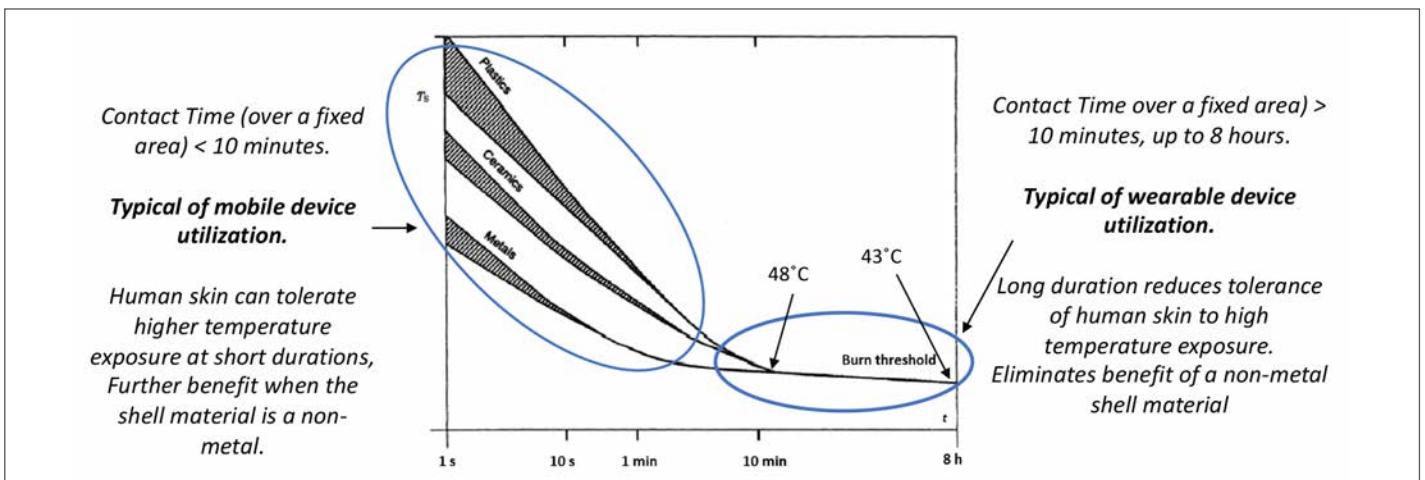


Figure 3 – Burn threshold temperature vs contact time for different device shell materials [4].

materials are associated with more efficient heat transfer to the skin and a higher risk of getting burned at a given combination of device temperature and contact duration.

These relationships are quantified in Figure 3, which was extracted from a widely used international standard [4]. The threshold level of severity assumed in this document is that of a second-degree burn.

This graph indicates that, for values of contact time less than a few minutes (typical of mobile device use), human skin can tolerate much higher device temperatures without burning than with longer contact times. Furthermore, as expected, the higher the thermal conductivity of the outer shell of the device, the shorter the time for a burn to occur at a given temperature.

However, for contact times > 10 minutes (typical of wearable devices) a burn can occur at much lower device temperatures (< 48°C) and the use of low-thermal-conductivity materials for the device shell no longer has a mitigating effect. For a contact time of 8 hours, a device temperature of only 43°C can result in a burn.

It is obvious that the mere avoidance of a burn is not enough to achieve a satisfactory user experience. To do this, the user should feel no discomfort at all. An extensive study, involving more than 70 adult subjects, has indicated that the threshold of pain can be avoided by maintaining device temperatures less than 39°C [5].

THERMAL LIMITS FOR IMPLANTABLE DEVICES

The process for determining whether an implantable device is within safety limits is a much more complicated process than that for portable and wearable devices.

To begin with, the role of thermal simulation is critical to perform an initial assessment of the viability of a given device embedded in a particular part of the human body. The simulations are supplemented by tests with animals and by *in vivo* testing in humans. As referred to in the discussion of the implantable glucose monitoring chip, the deployment of such a chip is greatly simplified if both the communication with the device and powering it up is done wirelessly. However, the fact that these electromagnetic waves are being transmitted through the body, results in the inductive heating of human tissue along the path of these E-M waves.

Hence, there are three sources of heat to be accounted for:

- Conductive heat transfer from the embedded device into the surrounding tissue
- Inductive heating of tissue along the path of the E-M waves
- Metabolic heat generation in a specific volume of tissue.

Additionally, there is a cooling mechanism due to the flow of blood through a volume of tissue referred to as perfusion.

The combined effect of these heating and cooling processes has to be accounted for in using the appropriate simulation methodologies. Once the temperature distribution throughout the portion of the body of interest is calculated, the results can be compared with various criteria, depending on the part of the body being affected.

The literature indicates that the following are acceptable limits are for most tissues in the body [6]:

- 2°C increase in the temperature of the affected tissue

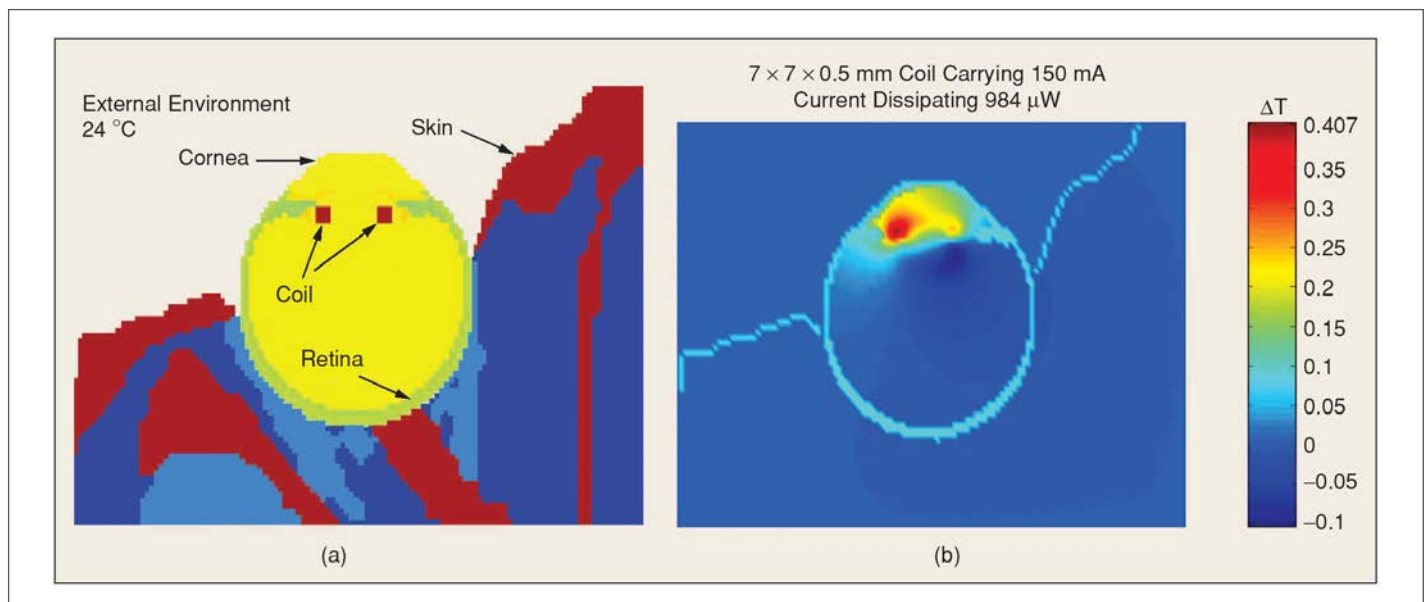


Figure 4 - Horizontal cross section through the center of the eye of the numerical head model. (a) Solid model showing the position of the implanted coil. Each tissue type is represented by a different color. (b) Thermal contour plot showing the temperature increase in the same cross section for a coil dissipating 984 μW. $\Delta T_{\max} = 0.407^{\circ}\text{C}$ [7].

- 40 mW/cm² heat flux flowing from the surface of the device into the surrounding tissue
- 1.6 mW/g of heating caused by the transmission of the E-M waves through the tissue of interest.
 - The standards documents, referred to this quantity as SAR (Specific Absorption Rate) [7].
- One exception is in the brain:
 - Very little is known about human cerebral tissue's response and tolerance to chronic exposure to a thermal stress from an implantable that generates low (<2°C) temperature changes [8].

THERMAL MODEL FOR THE TRANSFER OF IN THE HUMAN BODY

The Pennes bioheat equation is considered to be the standard in the field [6]. It was developed in 1948 by Harry H. Pennes. Because of the extensive use of this model, the required material properties have been measured for nearly all tissue types in the human body as well as for certain animals. It is essentially a time-dependent conduction model accounting for the three heating mechanisms just mentioned as well as the cooling effect of perfusion. However, its utility in many situations results from the wealth of material properties relevant to most of the types of tissue in the human body and in certain animals as well.

The Pennes equation is not discussed in detail here. However, some insight into the methodology can be gained to looking at thermal simulation results based on the method depicted in *Figure 4*.

The figure shows only part of a model of the entire head, with a retinal prosthesis mounted in the left eye, whose function is to partially restore sight in a visually impaired person. In the front of the prosthesis, there is an area-array photo sensor that communicates wirelessly with a retinal stimulating chip using a telemetry coil. This chip stimulates the retina by way of a microelectrode array attached to it. It should be noted that the model of the entire head includes 22 distinct types of tissue, each with its own thermal properties, metabolic rate, perfusion rate, etc. The E-M waves emitted by the telemetry coil heat up the surrounding tissue. The model calculates a maximum temperature increase of 0.41°C, which is within the allowable limit [9].

CONCLUSIONS

In the past 10 years, there have been significant advances in mobile and wearable devices. They are widely used in healthcare monitoring and fitness tracking. While there have been developments in implantable devices, they are still at the preliminary stages. However, they have the greatest potential to revolutionize healthcare by offering an always-on, web-enabled monitoring capability. Thermal characterization of these devices in an *in vivo* environment offers many challenges. Fortunately, they are being met by the rapid development of the necessary thermal tools.

REFERENCES

- [1] B. Guenin, "Wearable Electronics in Healthcare: Technology, Applications, and Challenges," Presented in panel session P2: Thermo-fluidic Challenges in Healthcare. iTherm Conference, 2018, San Diego
- [2] Report, World Health Organization (WHO) – "Global Report on Diabetes," 2016
- [3] J Walk, *et al.*, "Remote Powered Medical Implants for Tele-monitoring," Proceedings, IEEE, Vol. 102, No. 11, Nov. 2014
- [4] IEC GUIDE 117 -- Electrotechnical equipment – Temperatures of touchable hot surfaces Appendix A, 2010.
- [5] R. Defrin, I A. Ohry, N. Blumen, and G. Urca, "Sensory determinants of thermal pain," *Brain* (2002), 125, 501-510
- [6] Patrick D. Wolf, "Thermal Considerations for the Design of an Implanted Cortical Brain-Machine Interface (BMI)," Chapter 3 in, "Indwelling Neural Implants: Strategies for Contending with the In Vivo Environment," W. M. Reichert WM, editor, CRC Press, 2008. Available online at: <https://www.ncbi.nlm.nih.gov/books/NBK3932/>
- [7] IEEE Standard for Safety Levels with Respect to Human Exposure to Radio Frequency Electromagnetic Fields, 3 kHz to 300 GHz, IEEE Standard C95.1, 1999.
- [8] Huan Wang *et al.*, "Brain temperature and its fundamental properties: a review for clinical neuroscientists," *Frontiers in Neuroscience*, Vol. 8, p 307 (2014).
- [9] G Lazzi, "Thermal Effects of Bioimplants -- *Power Dissipation Characteristics and Computational Methods*," *IEEE Engineering In Medicine And Biology Magazine*, Sept./Oct. 2005.

A Figure of Merit for Smart Phone Thermal Management

Reprinted from Winter, 2015, issue

Victor Chiriac^{1*}, Steve Molloy¹, Jon Anderson¹, and Ken Goodson²

Author affiliations at time of original printing: 1 Qualcomm Technologies, Inc., 2 Stanford Mechanical Engineering.

*Victor Chiriac is currently with Futurewei Technologies (Huawei R&D USA) and is an Associate Technical Editor of this publication.

INTRODUCTION

With smart phones and other mobile devices available in a variety of sizes and shapes, it is challenging to think in a consistent and comparative manner about the effectiveness of the thermal management solutions that they employ. This is growing more important as the mobile and wireless industries and associated research communities explore novel mobile cooling approaches. Here we define a universal thermal figure of merit - a dimensionless *Coefficient of Thermal Spreading* (CTS) - that can be calculated using either numerical simulations or Infrared (IR) surface temperature imaging and can be used to compare the thermal design effectiveness of many mobile devices and power levels. The proposed CTS Figure of Merit quantifies the effectiveness of heat spreading within the device by means of the uniformity of the surface temperature, and addresses a long-time need to quantify the thermal design effectiveness of various mobile devices which are skin temperature limited.

There has been past work on thermal performance metrics of electronics, particularly those for which central processing unit (CPU) overheating limits power generation. Some metrics are defined at the package level for single or multi-chip designs, and are useful for junction temperature prediction and as performance figures of merit [1, 2]. Other authors discuss the importance of the skin cooling and other thermal challenges in handheld mobile devices [3, 4]. However, when it comes to the system level thermal performance, the industry lacks a metric to quantify the “goodness” of the thermal design. A key benefit of such a metric would be to track the impact of design changes on the thermal performance considering the device skin limits.

One major thermal challenge of portable electronic devices is the strong spatial and temporal variability of the thermal boundary conditions at the case. A phone with outstanding *internal* thermal management will likely aim for a reasonably consistent temperature on its *exterior* surfaces. In fact, in the limit of perfect internal

thermal management, all of the heat generated by the chips and other components inside the phone will be spread to the various phone surfaces and provide a nearly uniform temperature distribution when viewed from the outside. *Figure 1* shows that selecting a good thermal management strategy inside the phone improves the temperature uniformity and lowers the peak surface temperature.

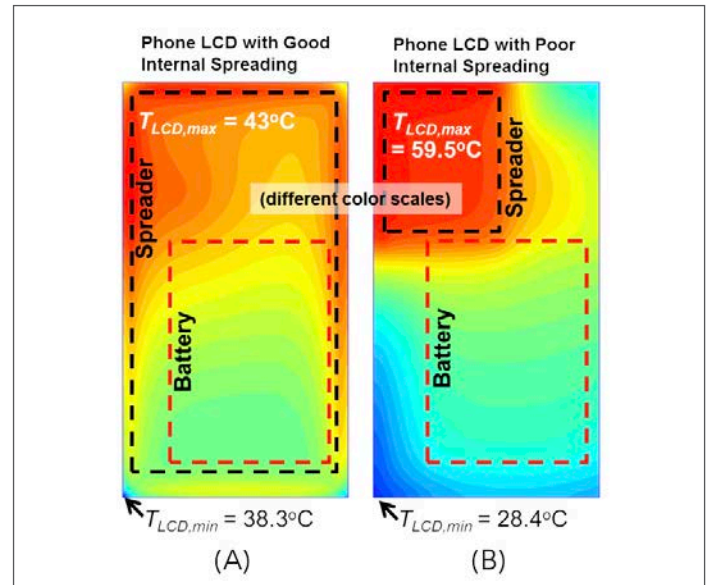


Figure 1. Simulated temperature distributions on the surface of a generic phone LCD (138 mm x 70 mm) for two different thermal management schemes. (a) Large heat spreader (128 mm x 62 mm), which couples the battery with the heat generating chips and yields a more uniform temperature. (b) Smaller heat spreader (35 mm x 33 mm) yielding highly nonuniform LCD temperature.

Figure 1 illustrates that phone thermal design must meet certain skin limit temperatures and avoid the potential hot spots. The poor heat spreading on the device surface leads to a peak temperature of 59.5°C (*Figure 1(b)*), violating the 45°C skin tempera-

ture limit specifications set for the current design. By improving the thermal spreading, the peak temperature drops below the critical limit (Figure 1(a)).

The new proposed spreading metric is important both for thermal and electrical design/performance. At present, to meet the various performance specifications (skin/junction limit temperatures), the processors are throttled to reduce the power that leads to exceeding the limits. It is in the interest of the chip/device manufacturers to come up with a system level solution that will increase the overall electrical and thermal performance. This prompted the need for a heat spreading metric.

DEFINING THE COEFFICIENT OF THERMAL SPREADING (CTS)

We define the specific figure of merit associated with the heat spreading efficiency, a metric which we will call the “Coefficient of Thermal Spreading” (CTS). This metric indicates that by designing towards improvements in the CTS, we can improve the heat spreading and enhance the power handling capacity of a given phone/mobile device, achieving higher performance.

Figure 1 suggests that the variation of the surface temperature is decreased as the thermal design quality improves. One strategy for defining the CTS would be to evaluate the standard deviation of the temperature about its average value, T_{ave} . The maximum temperatures depicted for the two phone designs in Figure 1 suggest the following:

$$CTS = \frac{\theta_{ave}}{\theta_{max}} = (T_{ave} - T_{ambient}) / (T_{max} - T_{ambient}) \quad (1)$$

Equation (1) is simply the ratio of the average temperature rise on the phone surface to the peak temperature rise. This ratio is dimensionless and increases to unity as the phone approaches a “perfect” thermal design, with uniform case temperature, for which T_{ave} and T_{max} are the same. In contrast to a metric based

on the standard deviation, Equation (1) is directly related to power and maximum surface temperature, the key inputs/deliverables of the design process. Improving the CTS translates directly into a reduction of the maximum surface temperature for a given power.

To develop a quantitative metric, it is useful to assume a constant value of the convective heat transfer coefficient, h , over the entire surface, in part because the local heat transfer rate varies due to a variety of external parameters. Equation (2) shows that for a given power and surface area, the average surface temperature is independent of the phone design. A poorly designed phone has hot/cold regions, but the average surface temperature is the same as of a well designed phone, assuming equal power generation and surface area for both devices.

$$P_{phone} = h A \theta_{ave} \quad (2)$$

where P_{phone} [W] is the total heat generated in the phone; A is the total surface area, and $\theta_{ave} = T_{ave} - T_{ambient}$ is the average phone surface temperature rise relative to the ambient air.

There is another way to calculate the CTS, which may be more straightforward depending on what information is available. Making use of Equation (2), we calculate the CTS using:

$$CTS = \frac{P_{phone}}{hA\theta_{max}} = \frac{P_{phone}}{P_{perfect}} \quad (3)$$

where P_{phone} is the power generated without rising above the case temperature limit and “ $P_{perfect/ideal}$ ” is the power removed from a phone with perfect internal spreading.

Equation (3) is useful for extracting the CTS from infrared imaging data, which can provide a solid estimate of the maximum temperature rise.

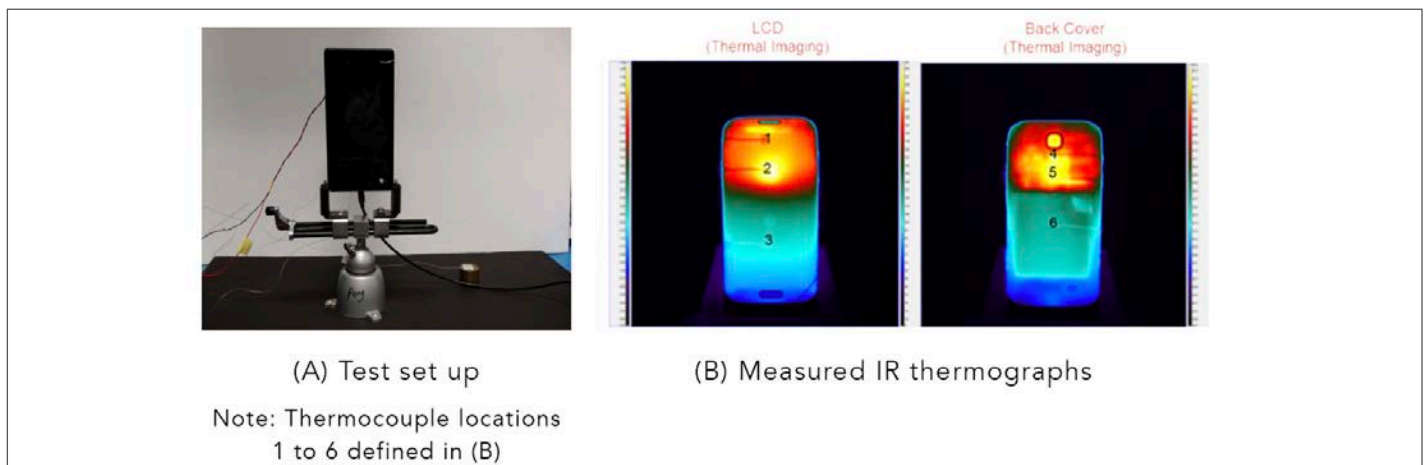


Figure 2. IR imaging of commercial phone.

MEASURING THE CTS

IR imaging was performed to gain understanding of the CTS metric. The benchmark use case is Quad-Dhrystone and the device is in vertical orientation (*Figure 2(a)*). Test details/equipment: a) K-type thermocouple measures the ambient temperature; b) data logger records the thermocouples temperatures; c) IR camera measures the LCD/Back Cover peak/average temperatures; d) Wait 40 mins until surface temperatures reach steady-state, start CTS measurement.

Since the surface emissivity of LCD/back cover is unknown, three K-type thermocouples (designated as 1 through 6, three on each LCD/Back cover surface) were mounted at low/medium/high-temperature zones at LCD/Back cover (*Figure 2(b)*). The thermocouple readings were used as the reference temperature to calibrate the emissivity of the LCD/Back cover surfaces. The surface emissivity setting of the IR camera is adjusted until the temperature difference between the thermocouple and IR camera reading is less than 1°C. The determined surface emissivity is the emissivity of the LCD/Back cover surface.

There is potential for further reduction in the tests variability (due to the open air environment) by using JEDEC closed box [5], with modified port for IR camera access. This deserves further evaluation, in case the industry is moving towards the CTS concept adoption.

To capture the temperature profiles: a) Run power intensive use case; b) Capture the surface temperature using IR camera; c) Port the IR temperature data into .csv file; d) Do an area weighted average of the surface temperatures for the display/case surfaces; e) Extract the overall device skin maximum temperature; f) Calculate $CTS = (T_{ave} - T_{ambient}) / (T_{max,skin} - T_{ambient})$. *Figure 3* summarizes the CTS measurement over 30 minute: CTS peaks at 0.62 for this specific device.

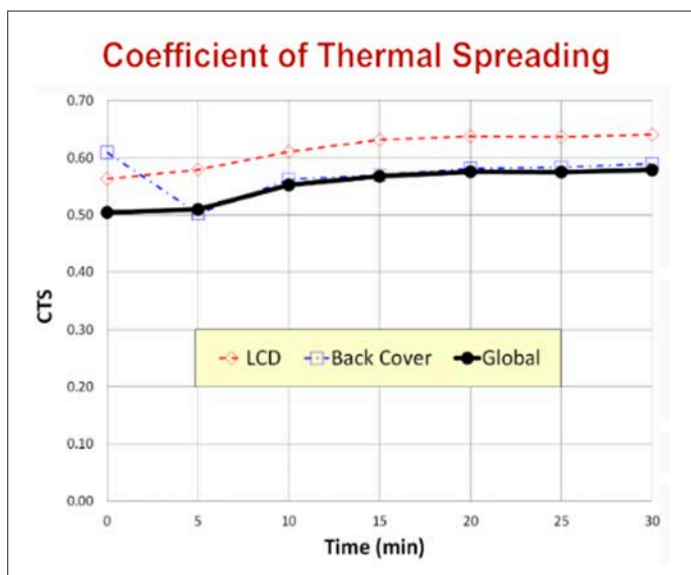


Figure 3. Calculated Coefficient of Thermal Spreading extracted experimentally for commercial phone

EXAMPLE APPLICATIONS OF THE COEFFICIENT OF THERMAL SPREADING (CTS)

We expect the CTS to guide the design improvements and interactions with the phone/mobile manufacturers/companies. We completed several simulation/CFD studies of phone design incorporating differing spreader geometries, at various powers. *Figure 4* plots the simulated maximum surface temperatures as a function of heat spreader geometry and power.

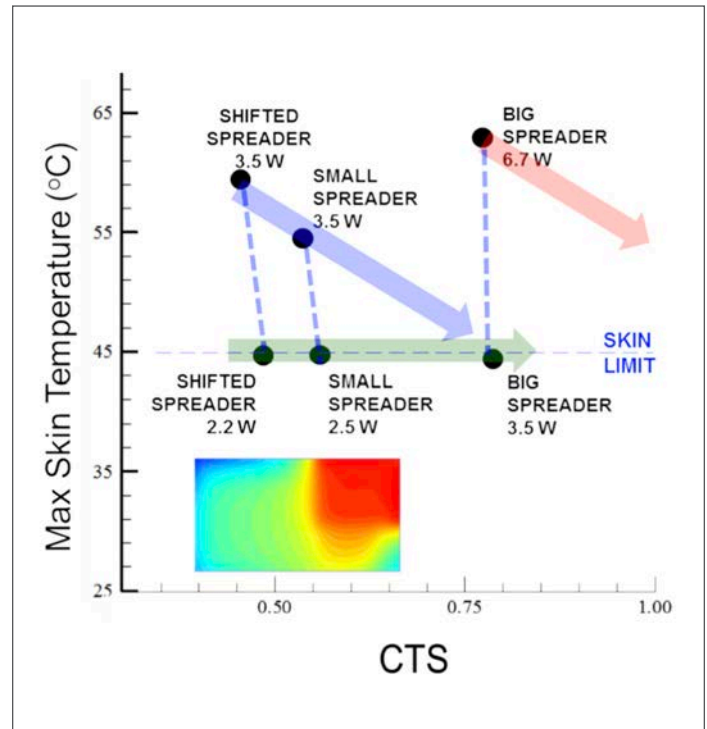


Figure 4. Maximum skin temperature versus CTS. Note: (i) The phone designs along the green arrow are limited by skin temperature, with power chosen specifically to meet that limit. (ii) The designs along the blue arrow show what happens to the skin temperature, for a constant given power, through improved thermal design. (iii) The red arrow suggests that it is impossible to improve a design sufficiently to cool very large power loads.

For a phone that is cooled sufficiently well, increasing the CTS guides to higher power capacity without overheating the case. In *Figure 4*, the green arrow draws attention to three successive simulations for increasing spreader size that allow the power to be increased from 2.2 to 3.5 W without overheating the skin. Larger spreaders allow the CTS to increase from 0.5 to 0.8. By increasing the CTS of a device from 0.5 to 0.8, there is over 1.2W Power benefit and the skin limit stays at 45°C.

For problem phone designs (device skin is too hot), increasing the CTS should guide to a working design, or to the conclusion that the power is unmanageable. The blue arrow in *Figure 4* draws attention to three successive simulations at 3.5W constant power, for which increasing the spreader size (thus increasing the CTS) drops the maximum skin temperature from ~ 60°C to the required 45°C limit.

For the case of 6.7W and the big spreader, the red arrow suggests that the CTS needs to be increased above unity to function properly. This is impossible, as the CTS reaches a maximum of one for a perfect/isothermal case, meaning that power reductions will be essential. For that specific device platform, the maximum power using an ideal CTS is limited to 3.8W.

Finally, the CTS is a figure of merit for the design geometries/materials, and should be independent of the power level for the given use case/s. The dashed blue lines in Figure 4 show that, for a given spreader dimension, the CTS is essentially independent of the phone power. The dashed lines are not perfectly vertical because of the slight temperature dependence of the thermal properties.

Although the CTS is power independent for specific use case/s, the CTS does vary with time. If Equation (1) is evaluated as a function of time, while the device is heating up, the CTS evolves with time and approaches higher degree of uniformity in steady state. The CTS remains largely independent of power levels, although this can become more complicated if the power is time varying as well.

QUANTITATIVE DESIGN TARGETS USING THE CTS

The CTS is a powerful tool as it enables the best performing mobile/portable electronic devices. Chip manufacturers can define a minimally acceptable CTS level to ensure that their chips are cooled appropriately and deliver a level of performance that customers will find compelling/favorable. While all companies should strive for a CTS approaching unity (the perfectly cooled phone/mobile), eventually the costs associated with internal thermal management may become excessive. With improvements in thermal technologies, the higher CTS/performance devices should increase.

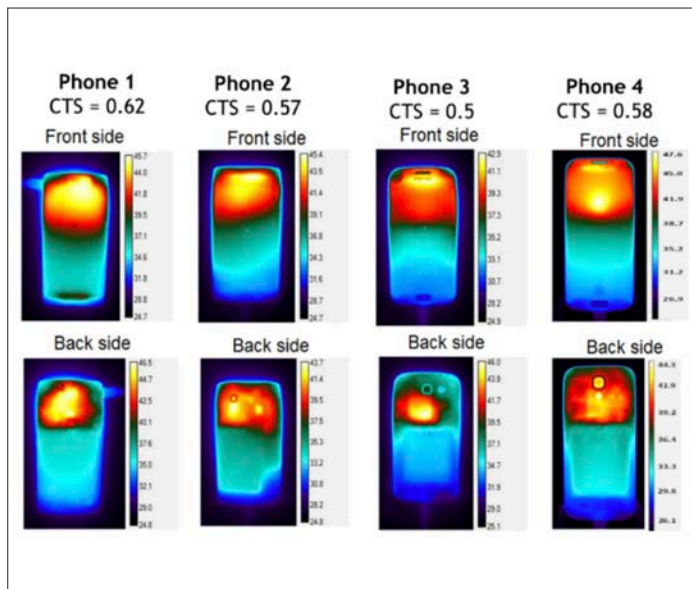


Figure 5. Measured IR temperature surface thermographs and CTS values for several commercial phones. CTS calculated using Equation (3) and the infrared imaging data. The temperature scale is different for each phone.

Our internal thermometry work has evaluated CTS values from 0.5 to 0.62 for various commercial phones (Figure 5): these numbers are critical because they translate directly into allowable internal power generation levels. By encouraging the phone manufacturers to increase the CTS to higher levels – our simulations suggest 0.8 – it is possible to achieve better balance between performance and cost.

WHY IS THE CTS IMPORTANT?

The increased CTS leads to better heat transfer and reduced peak temperature at the phone surface. As the internal spreading improves (CTS from 0.43 to 0.84), the device skin temperatures drop below the critical values (no hot spot) and a smaller temperature gradient occurs across the device surface/s (Figure 6). The high CTS device dissipates an extra 1.2W before it violates the skin limits compared to the design with low spreading efficiency (CTS = 0.43).

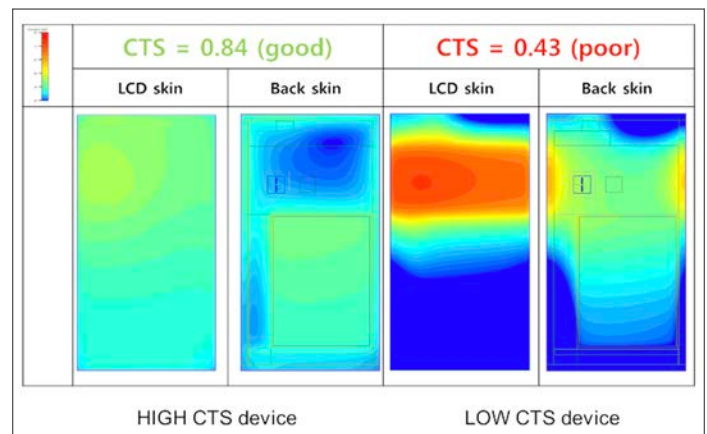


Figure 6. Comparison of calculated CTS values for poorly designed (CTS = 0.43) versus well designed (CTS = 0.84) devices: hot spot evident on poorly designed vs well spread heat on well designed phone skins. Note: CTS calculated using Equation (1) with average/peak skin temperatures from simulations. The temperature scale is the same.

For the specific device tested/simulated: every 1°C skin temperature difference leads to 0.16 W change in power, and is achieved by reducing CTS by 0.03.

HOW CAN WE IMPROVE THE CTS?

To enhance the mobile device heat spreading (CTS): a) Optimize the PCB ground plane; b) Use larger copper content for solid ground plane layer; c) Connect all ground pins of key ICs directly to this layer; d) Separate hottest ICs; d) No high Power ICs overlap on opposite PCB sides; e) Place connectors on opposite sides of key ICs where possible.

ALTERNATIVE CTS FORMULATIONS?

The authors evaluated alternative CTS formulations: a) T_{avg}/T_{max} ; b) T_{max}/T_{ideal} ; c) T_{ideal}/T_{max} ; d) $T_{ideal_system}/T_{real_system}$. Due to the lack of a physical meaning or independence on ambient Temperatures, it was decided to select the most appropriate version, as defined by Equation (1).

CONCLUDING REMARKS

This article proposes a new, dimensionless thermal spreading effectiveness metric for mobile devices, named CTS (Coefficient of Thermal Spreading). The CTS value quantifies the internal thermal spreading of mobile devices, and is a specific metric to improve the thermal design. It indicates how much a given mobile device can be improved for the given shape/size/form factor. As shown by simulations, optimally designed phones could reach CTS values between 0.8 and 0.9, while poorly balanced phones have CTS values below 0.5. Different mobile devices have different CTS values depending on overall size and internal design. CTS metric is used to help improve the thermal spreading over the device surface and reduce the skin maximum temperature. If adopted by the industry, the CTS Figure of Merit will lead to more thermally balanced phones/mobile devices.

ACKNOWLEDGEMENT:





The authors appreciate the help of Qualcomm San Diego team members: Luis Rosales performed the simulations, while Peng Wang took the thermometry data. Many other people provided valuable feedback and expertise.

REFERENCES

- [1] Guenin, B., "Toward A Thermal Figure Of Merit For Multi-Chip Packages" Calculation Corner, Electronics Cooling, Vol. 12, No. 4, November, 2006.
- [2] JEDEC document JESD51-12, "Guidelines for Reporting and Using Electronic Package Thermal Information." Available for download at www.jedec.org.
- [3] Mongia, R., Bhattacharyab, A., and Pokharna, H., "Skin Cooling and Other Challenges in Future Mobile Form Factor Computing Devices", Microelectronics Journal, Vol. 39, pp. 992 – 1000, 2008.
- [4] Lee, J., Gerlach, D.W., Joshi, Y.K., "Parametric Thermal Modeling of Heat Transfer in Handheld Electronic Devices", Proceedings of the 11th Intersociety Conference on Thermal and Thermomechanical Phenomena in Electronic Systems (ITHERM 2008), pp 604-609, 2008
- [5] JEDEC document JESD51-2A, "Integrated Circuits Thermal Test Method Environmental Conditions – Natural Convection (Still Air)." Available for download at www.jedec.org

2019 Company Products & Services Directory

In this section, we provide a quick guide to some of the top suppliers in each EMC category - in heat sinks, thermal testing, design services, and more. To find a product that meets your needs for applications, frequencies, standards requirements, etc., please search these individual supplier websites for the latest information and availability. If you have trouble finding a particular product or solution, email info@lectrixgroup.com for further supplier contacts.

COMPANY		CONTACT INFORMATION	PRODUCTS & SERVICES	
MEDIA PROVIDER SPOTLIGHT		LECTRIX 1000 Germantown Pike Plymouth Meeting, PA 19462 t: (484) 688-0300 w: www.lectrixgroup.com	- Strategy Firm - Full-Service Marketing - Publishing	- Events and Webinars - Custom Solutions - Training and Consultation
		Thermal Live™ 2019 Online Event October 22 nd - 23 rd 2019 t: (484) 688-0300 e: info@electronics-cooling.com w: www.thermal.live	- Training Seminars & Workshops	
COMPANY		WEBSITE	PRODUCTS & SERVICES	
A	Aavid Thermal Division of Boyd Corporation	www.boydcorp.com	- Blowers/Fan Accessories - Blowers - Chillers - Cold Plates - Fans - Gap Pads & Fillers	- Heat Pipes - Heat Sinks - Interface Materials - Liquid Cooling - Thermal Design Services - Thermal Testing
		www.alphanovatech.com	- Coolers - Heat Sinks - Thermal Design Services	- Thermal Tapes - Thermal Testing
	Ansys, Inc.	www.ansys.com	- Software	
B	Bergquist, a Henkel Company	www.bergquistcompany.com	- Gap Pads & Fillers - Interface Materials - Phase Change Materials	- Substrates - Thermal Tapes
C	Celsia Inc.	www.celsiainc.com	- Heat Pipes - Heat Sinks - Heat Spreaders	- Thermal Design Services - Vapor Chambers
	CPC Worldwide	www.cpcworldwide.com	- Connectors	
	COFAN U.S.A.	www.cofan-usa.com	- Blowers - Coolers - Fans	- Heat Sinks - Heat Pipes - TIM's
D	DegreeC, Degree Controls Inc.	www.degreec.com	- Sensors, Test & Measurements	
		www.deltabreez.com	- Blowers - Fan Trays	- Fans - Heat Exchangers
E	ElectronicsCooling®	www.electronics-cooling.com	- Media	- Training Seminars & Workshops
	Element Six	www.e6.com	- Heat Spreaders	

COMPANY		WEBSITE	PRODUCTS & SERVICES	
F	Fujipoly® America Corp.	www.fujipoly.com	- Connectors - Gap Pads & Fillers	- Interface Materials - Thermal Design Services
H	Heilind Graphics Corporation	www.heilind.com	- Liquid Cold Plates	
I	Institution of MECHANICAL ENGINEERS	www.imeche.org	- Training Seminars & Workshops	
	International Manufacturing Services, Inc. (IMS)	www.ims-resistors.com	- Heat Spreaders	- Thermal Management Devices
J	JARO Thermal	www.jarothermal.com	- Blowers - Fans - Heat Pipes	- Heat Sinks - Vapor Chambers
L	Laird Technologies	www.lairdtech.com	- Phase Change Materials	- Thermoelectric Coolers
	Leader Tech	www.leadertechinc.com	- Gap Pads & Fillers	
	LMB Fans	www.lmbfans.com	- Fans	
M	Malico	www.malico.com	- Cold Plates - Heat Sinks	- Liquid Cooling
	Master Bond, Inc.	www.masterbond.com	- Interface Materials	
	Mentor Graphics	www.mentor.com/mechanical	- Software - Thermal Design Services	- Thermal Testing
	Mersen	www.mersen.us	- Heat Pipes - Heat Sinks	- Liquid Cold Plates
N	NeoGraf Solutions	www.neograf.com	- Expandable Graphite - Flexible Graphite	- Heat Spreaders - TIM's
O	ORION Fans	www.orionfans.com	- Blowers/Fan Accessories - Fan Controllers - Fan Filters	- Fan Trays - Fans
P	Panasonic	na.industrial.panasonic.com	- Interface Materials	
	Polymer Science Inc.	www.polymerscience.com	- Gap Fillers - Heat Spreaders	- Interface Materials - Phase Change Materials
R	Rogers Corporation Advanced Connectivity Solutions	www.rogerscorp.com/acs	- Adhesives - Bonding	- Epoxy
	Rosenberg USA, Inc.	www.rosenbergusa.com	- Blowers - Fan Filters	- Fans
S	Semi - Therm	www.semi-therm.org	- Training Seminars & Workshops	
	Shin-Etsu MicroSi	www.microsi.com	- Interface Materials	
	Shiu Li Technology Co., LTD	www.shiuli.com.tw	- Interface Materials	- Thermal Tapes
	SIEMENS <i>Ingenuity for life</i>	www.siemens.com/mdx	- Education Courses/Seminars	- Software
	Staubli Corporation	www.staubli.com	- Connectors - Couplings	- Software
T	T-global Technology Co. Ltd	www.tglobal.com.tw	- Gap Pads & Fillers - Interface Materials	- Thermal Tapes
	Thermal Engineering Associates Inc.	www.thermengr.com	- Thermal Test Chips	
	TECA ThermoElectric Cooling America Corporation	www.thermoelectric.com	- Air Conditioners - Cold Plates	- Coolers - Thermoelectric Coolers
	Techsil Limited	www.techsil.co.uk	- Thermal Management Materials	
W	Wavelength	www.teamwavelength.com/	- Temperature Controllers	

Index of ADVERTISERS



Alpha Novatech, Inc.
473 Sapena Ct. #12,
Santa Clara, CA 95054

t: (408) 567-8082
e: sales@alphanovatech.com
w: www.alphanovatech.com
page: 2



CPC Worldwide
1001 Westgate Drive
St. Paul, MN 55114

t: (651) 645-0091
w: www.cpcworldwide.com
page: 21



LECTRIX
1000 Germantown Pike
Plymouth Meeting, PA 19462

t: (484) 688-0300
e: info@lectrixgroup.com
w: www.lectrixgroup.com
page: 44



Master Bond, Inc
154 Hobart Street
Hackensack, NJ 07601

t: (201) 343-8983
e: main@masterbond.com
w: www.masterbond.com
page: 28



Mentor Graphics
8005 SW Boeckman Road
Wilsonville, OR 97070

t: (800) 592-2210
e: sales_info@mentor.com
w: www.mentor.com
page: 5



NeoGraf Solutions, LLC
11709 Madison Avenue
Lakewood, OH 44107

t: (216) 529-3777
w: www.neograf.com
page: 14



SEMI-THERM 36
March 16th – 20th, 2020
Double Tree by Hilton
San Jose, CA 95110

t: (408) 840-2354
e: drael@semi-therm.org
w: www.semi-therm.org
page: 8



Thermal Live™ 2019
Online Event
October 22nd – 23rd, 2019

t: (484) 688-0300
e: info@electronics-cooling.com
w: www.thermal.live
page: 17

Call for Authors and Contributors!

Want to be a part of the next issue of Electronics Cooling? Have an article or blog post you'd like to write for Electronics-Cooling.com?

Let us know at
editor@electronics-cooling.com

 **electronics
COOLING**

www.Electronics-Cooling.com

From the Creators of *Electronics Cooling*

INTRODUCING



LECTRIX

THERE'S ONLY ONE SPOTLIGHT

ARE YOU IN IT?

Positioning Ambitious B2B Electronics Companies
for Aggressive Growth



www.lectrixgroup.com

PHILADELPHIA, PA | HONG KONG